

1 **ARTICLE**

2

3 **Revisiting Antarctic ice loss due to marine**
4 **ice cliff instability**

5

6 Tamsin L. Edwards* [a], Mark Brandon [b], Gael Durand [c], Neil R. Edwards [b], Nicholas
7 R. Golledge [d, e], Philip B. Holden [b], Isabel Nias [f], Antony J. Payne [g], Catherine Ritz
8 [c] and Andreas Wernecke [b].

9 * Corresponding author

10

11 a Department of Geography, King's College London

12 b School of Environment Earth and Ecosystem Sciences, Faculty of Science, Technology, Engineering and
13 Mathematics, Open University, Walton Hall. Milton Keynes, UK

14 c Univ. Grenoble Alpes, CNRS, IRD, IGE, F-38000 Grenoble, France

15 d Antarctic Research Centre, Victoria University of Wellington, Wellington 6140, New Zealand

16 e GNS Science, Avalon, Lower Hutt 5011, New Zealand

17 f Earth System Science Interdisciplinary Center, 5825 University Research Court, Suite 4001, College Park,
18 Maryland 20740-3823, USA

19 g Centre for Polar Observation and Modelling, School of Geographical Sciences, University of Bristol,
20 University Road, Bristol BS8 1SS, UK

23 **Predictions for sea-level rise from Antarctica this century range from zero to over one**
24 **metre. The highest are driven by the controversial ‘marine ice cliff instability’ (MICI)**
25 **hypothesis, where coastal ice cliffs rapidly collapse after ice shelves disintegrate from**
26 **surface and sub-shelf melting caused by global warming. But the MICI mechanism has**
27 **not been observed in the modern era, and it remains unclear whether or not it is**
28 **required to reproduce sea-level variations in the geological past. Here we quantify ice**
29 **sheet modelling uncertainties for the original MICI study and show the probability**
30 **distributions are skewed towards lower values (most likely value: 45 cm under very**
31 **high greenhouse gas concentrations). However, MICI is not required to reproduce sea-**
32 **level changes in the mid-Pliocene, Last Interglacial or 1992-2017, and without it the**
33 **results agree with previous studies (all 95th percentiles are less than 43 cm). We**
34 **therefore find previous interpretations of the MICI projections over-estimate sea-level**
35 **rise this century. The hypothesis is not well constrained: confidence in projections with**
36 **MICI would require a greater diversity of observationally constrained models of ice**
37 **shelf vulnerability and ice cliff collapse.**

38 Projections of the Antarctic contribution to global mean sea-level rise this century from
39 process-based models vary widely¹⁻⁶. In particular, DeConto and Pollard (2016)⁶ (here DP16)
40 introduced a hypothesised ‘marine ice cliff instability’ (MICI) process⁷ resulting in mean
41 values exceeding 1 m by 2100 under some methodological choices. However, the DP16
42 results are sensitive to these choices (Table 1: Mean \pm 1 s.d.; Extended Data Figures 1a and
43 b), and the shapes of the probability distributions are very poorly known (Extended Data
44 Figure 2), leading to extremely wide probability intervals (Table 1). This considerable
45 uncertainty poses challenges for robust and cost-effective coastal flood risk management.

46 The Antarctic contribution to global mean sea-level (GMSL) has two parts: increasing
47 snowfall, which is expected to reduce GMSL by a few centimetres this century, and ice
48 discharge into the ocean, which is very uncertain¹. The latter is determined by outflow of ice
49 across the ‘grounding line’ (the boundary between floating and grounded ice), which can
50 increase due to faster ice flow or inland retreat of the grounding line. Ice discharge can
51 increase if buttressing by ice shelves is reduced by (1) ice shelf thinning, caused by enhanced
52 oceanic melting due to circulation changes⁸ or direct warming, or (2) partial or total ice shelf
53 collapse, caused by widening of surface crevasses by meltwater due to atmospheric
54 warming^{9,10}.

55 Marine parts of the ice sheet, lying on bedrock below sea-level, are potentially
56 vulnerable to two hypothesised positive feedbacks that may have led to past collapse of the

57 West Antarctic ice sheet¹¹. Both are based on physical mechanisms with theoretical
58 foundations, but it is not yet clear the degree to which these could lead to positive feedbacks
59 (i.e. widespread, rapid and sustained ice losses). ‘Marine Ice Sheet Instability’ (MISI)¹² is a
60 self-sustaining retreat of the grounding line in regions where the bedrock slopes downward
61 inland, triggered by ice shelf thinning or collapse. Ice thickness at the grounding line
62 increases (due to the bedrock slope), leading to faster ice flow, causing further retreat.
63 Satellite and modelling evidence suggests MISI is underway in West Antarctica^{13,14,15}, though
64 it is unclear the degree to which the driver of this, warm Circumpolar Deep Water breaching
65 the continental shelf, has been affected by human activities^{1,16,17}. ‘Marine Ice Cliff Instability’
66 (MICI)^{6,7} is a self-sustaining retreat of the ice front in regions where the ice is 100 m or more
67 above the ocean surface¹⁸, triggered by ice shelf collapse. These tall ice cliffs are structurally
68 unstable, and their collapse could leave behind further tall cliffs, resulting in sustained ice
69 losses. Observational evidence for MICI is indirect: an absence of ice cliffs taller than 100 m,
70 and rapid retreat of the front of the Jakobshavn (Greenland) and Crane (Antarctic) glaciers
71 (see Knowledge Gaps and Future Directions).

72 DP16⁶ use an Antarctic ice sheet model with a new parameterisation of MICI⁷,
73 generating a 64-member ensemble by varying three parameters controlling the relationship
74 between ocean temperature and basal melting, ice shelf disintegration, and maximum rate of
75 ice cliff collapse. They make projections to 2500 under three Representative Concentration
76 Pathways (RCPs): RCP2.6, RCP4.5 and RCP8.5, for very low, low-to-medium and very high
77 greenhouse gas concentrations respectively¹. They calibrate these by accepting only ensemble
78 members that reproduce reconstructed Antarctic sea-level contributions in the mid-Pliocene
79 (~3 million years ago) and Last Interglacial (LIG: ~130,000–115,000 years ago) eras, and
80 present results for two methodological choices. The first is the Pliocene calibration, using an
81 interval of 5-15 m or 10-20 m; the latter increases sea-level contributions by up to 40 cm by
82 2100 and 2.5 m by 2500 under RCP8.5 (here “LowPliocene”/“HighPliocene”). The second is
83 an ocean temperature correction of +3°C in West Antarctica to improve simulations of the
84 present ice sheet (“BiasCorrected”/“BiasUncorrected”); this increases sea-level contributions
85 by up to 15 cm this century, but makes little difference by 2500. Results for RCP8.5 at 2100
86 are given in Table 1; the corresponding distributions are shown in Extended Data Figure 2.

87 We use statistical techniques for quantifying uncertainties for computationally
88 expensive computer models to re-examine, and estimate probability distributions for, the
89 DP16 projections. We calibrate with the Pliocene, LIG and satellite (1992-2017) eras and
90 make probabilistic projections with and without MICI, comparing with other probabilistic

91 model projections and a Gaussian interpretation of DP16. Finally, we outline knowledge gaps
92 and suggest future directions.

93

94 **New projections for Antarctica**

95 We estimate probabilistic projections for the Antarctic contribution to sea-level rise by
96 ‘emulating’ the DP16 ice sheet model (see Methods). This quantifies how a computer
97 model’s outputs vary as a function of its input parameters, to predict outputs for any
98 parameter values, enabling us to generate a far larger ensemble than with the original model
99 and to present results both with and without MICI. For this we assume all parameter values
100 are equally likely within the original ranges, based on discussions with the DP16 authors (R.
101 DeConto, pers. comm.). Estimating probability distributions allows meaningful comparison
102 with other studies, and decision-making using sea-level exceedance probabilities under both
103 MICI and No-MICI scenarios. Our method has two further additions: calibration with both
104 palaeodata and satellite data, re-expressing this in the statistical framework of ‘history
105 matching’ (see Methods), and accounting for ice sheet model error.

106 Reconstructions of past climate change provide important tests of models, particularly
107 when the changes were large and/or warmer than today, but their uncertainties are typically
108 large and often poorly-defined¹⁹; recent observations have smaller signals but far smaller
109 uncertainties. The two provide complementary information, so we use both. We use the
110 LowPliocene (equivalent to a combined range of 5-20 m, because the highest simulation is
111 12.4 m), for two reasons: the large reconstruction uncertainty (values lower than 10 m cannot
112 be ruled out: e.g. a more recent estimate has a maximum of 13 m²⁰), and because the DP16
113 projections are very sensitive to the lower bound of the HighPliocene (Extended Data Figure
114 2a and b). The ‘calibration relationships’ between RCP8.5 sea-level contribution at 2100 and
115 sea-level change for the three past eras are shown in Extended Data Figure 3.

116 To estimate probability distributions we use ‘history matching’ (HM), where
117 implausible model versions are excluded, rather than the more commonly known Bayesian
118 calibration (BC), where model versions are weighted by their agreement with observations
119 using a likelihood function (metric of model success). This is for several reasons. The
120 concept of HM is the same as DP16, which allows us to make a simpler and more transparent
121 comparison. This method effectively estimates what DP16 would have found if they had
122 substantially greater computing resources, calibrated their ensemble with satellite data, and
123 accounted for model error. History matching is also more ‘cautious’ than Bayesian model

124 calibration: if no model versions match the data, they are all excluded, while BC retains all
125 and upweights the ‘least bad’. Finally, we do not know the shape of the crucial Bayesian
126 likelihood function for the Pliocene and LIG: this would require estimates of the palaeodata
127 mean and error distribution, rather than assuming all values within the interval are equally
128 likely. Guessing these might shift (wrong mean) or narrow (wrong distribution) the final
129 probability distributions.

130 Accounting for model error, ‘discrepancy’²¹, widens the calibration intervals of
131 acceptance (Extended Data Figures 3 and 4: from grey shaded boxes to dashed lines) and is
132 necessary to avoid over-confidence^{22,23}: the aim is to account for model structural error and
133 other model uncertainties not sampled in the ensemble. These discrepancy terms are
134 tolerances that reflect how well we expect the ice sheet model to reproduce reality. We
135 specify them using expert judgement, including the judgement that they are greater than
136 reconstruction/observation errors^{4,24} (i.e. we judge that confidence in simulating reality with
137 the ice sheet model is lower than in observing or reconstructing it from measurements).
138 Reconstruction errors are not defined by DP16, so we conservatively use half the palaeodata
139 range to avoid underestimating uncertainty (Pliocene: 5 m; LIG: 2 m). For the satellite period,
140 the sea-level change is (0.756 ± 0.386) cm for 1992-2017²⁵; we conservatively specify the
141 model error as 0.5 cm.

142 We present projections at 2100 in Figure 1 and Table 2. The distributions are skewed:
143 modes are consistently lower than medians and means. The results are not strongly dependent
144 on the Pliocene calibration lower bound, unlike the DP16 ensemble, due to the much larger
145 ensemble size (Extended Data Figure 2c: RCP8.5 at 2100 with MICI). Emulated projections
146 without MICI are much lower than those with MICI, and are consistent with previous
147 projections by Ritz et al. (2015)⁴ (Figure 1b). The results are robust to changes in calibration
148 era and discrepancy (Extended Data Figure 5).

149 Crucially, our results show ice cliff instability is not required to reproduce sea-level
150 changes in these three very different eras: 55% of the MICI and 51% of the No-MICI
151 emulator ensemble members simultaneously pass calibration with the Pliocene, LIG and
152 satellite eras (Extended Data Figure 4: larger emulator blue circles within dashed box). MICI
153 increases the ensemble range to encompass more of the data intervals, but the emulator can
154 identify many more areas of the model’s parameter space that are successful: including many
155 without MICI. MICI is therefore not necessary for realistic simulations of these periods, so
156 this positive feedback hypothesis cannot be confirmed or ruled out with this data and
157 calibration method. In fact, the Pliocene does not rule out any ensemble members, because

158 accounting for model error widens the calibration interval to accept them all (Extended Data
159 Figure 3a).

160 The original DP16 projections have substantial probabilities of net sea-level fall this
161 century, with the RCP8.5 LowPliocene mean \pm 1 s.d. envelope including negative values
162 until the 2070s. The emulated projections reflect this (Figure 2), though with lower
163 probability (5th percentile negative until the 2070s). Calibration selects mostly positive sea-
164 level contributions during 1992-2017 (Extended Data Figure 3c), then surface accumulation
165 increases with warming (particularly for RCP8.5) and dominates over ice discharge in many
166 ensemble members during this period.

167 We estimate when the hypothesised MICI feedback would accelerate sea-level rise.
168 Contributions with MICI quickly start to diverge from those without for all RCPs: in the
169 2020s (95th percentiles: Figure 2), resulting from the Antarctic Peninsula (DP16: Figure 4c).
170 Dependence of the Antarctic contribution on RCP with MICI begins mid-century, while
171 emergence of a clear, RCP-dependent signal without MICI begins in the 2060s-2070s.

172 We apply the same emulation and calibration methods to the full DP16 time series
173 (Figure 3a). The RCP8.5 distribution remains very skewed, with the mode at the low end of
174 the range; the same is true of RCP4.5, until the 2340s when the mode jumps to the high end
175 of the distribution (from 1.7 m to 4.6 m) and remains there (as seen for 2500). Virtually all
176 the long-term uncertainty arises from MICI. The No-MICI projections remain narrow over
177 multiple centuries – particularly for RCP8.5, which becomes more narrow – because the sea-
178 level contribution in the DP16 ensemble depends less on the parameters controlling ice shelf
179 vulnerability and basal melting over the long-term than during this century. This suggests the
180 DP16 ensemble either seriously under-samples model uncertainties relevant to long-term
181 change, or the model is structurally deficient because the sensitivity to important parameters
182 diminishes under warming. We therefore consider the post-2100 projections to be less
183 reliable.

184 The projected probabilities of exceeding 1 m sea-level contribution over time are shown
185 in Figure 3b. These show that, for high probabilities of first exceeding 1 m Antarctic
186 contribution to sea-level, the difference in exceedance time between RCP8.5 and RCP4.5
187 greenhouse gas concentration scenarios is generally much greater than between projections
188 with or without MICI under RCP8.5. They also show that RCP2.6, i.e. strong mitigation of
189 greenhouse gas concentrations broadly consistent with the 2015 Paris Agreement, is the only
190 one of these scenarios to ensure a low probability of high sea-level rise.

191

192 **Multi-model comparisons**

193 Figure 4 compares the emulated projections at 2100 under RCP8.5 and RCP2.6 with other
194 studies. We compare only with probabilistic projections²⁻⁵, because these have a clear
195 interpretation, and studies that incorporate at least some process-based modelling (rather than
196 only expert elicitation or extrapolation), because we are interested in physical modelling
197 uncertainties and we expect the Antarctica to be governed by different processes in the future
198 than the past (which is not accounted for in extrapolation).

199 We find the emulated No-MICI results agree well with other studies: 95th percentiles
200 are around 30-40 cm under high scenarios and 10-20 cm under low scenarios, despite the use
201 of very different models and approaches (and some differences in scenario and contribution
202 definitions; see Methods). A recent projection by Golledge et al. (2018)²⁶ incorporating ice-
203 ocean-atmosphere feedbacks is also consistent (14 cm under RCP8.5. compared with DP16-
204 based median of 15 cm; emergence of signal from mid-century). The No-MICI projections
205 for RCP4.5 are very similar to the IPCC (2013) assessment for 2100 relative to 1986–2005¹
206 (Emulated DP16: 5 [–1, 15] cm median and 66% probability interval; IPCC: 5 [–5, 15] cm
207 median and 66% or greater probability). The IPCC (2013) estimates for Antarctic ice
208 discharge do not depend on greenhouse gas scenario, so the projections for RCP2.6 are
209 slightly lower than the IPCC (Emulated DP16: –1 [–7, 7] cm, IPCC: 6 [–4, 16] cm) and
210 higher for RCP8.5 (Emulated DP16: 21 [13, 31] cm, IPCC: 4 [–8, 14] cm).

211 Le Bars et al. (2017)²⁷ make probabilistic interpretations of DP16 for assessing high-
212 end total GMSL by taking the HighPliocene BiasCorrected mean and standard deviation and
213 assuming the distribution is Gaussian. This gives probabilities of exceeding 0.5 m and 1 m
214 Antarctic contribution by 2100 under RCP8.5 of 96% and 65%, respectively. We argue this
215 interpretation is not justifiable, as the original DP16 distributions are skewed (Extended Data
216 Figure 2) and the HighPliocene constraint is not robust (discussed above). Using minimal
217 assumptions about the distribution shape instead would mean probability intervals were very
218 poorly constrained (Table 1). Our estimates of the distribution shape give lower exceedance
219 probabilities: 71% and 36%, respectively (Table 2); We conclude that, although significant
220 sea-level rise is possible under the probability distributions estimated from DP16, Le Bars et
221 al. (2017) systematically overestimate the probability of high sea-level contribution from
222 Antarctica this century.

223 Only Ritz et al. (2015)⁴ have made probabilistic projections beyond 2100. At 2200, the
224 emulated No-MICI projections under RCP8.5 are an order of magnitude higher than Ritz et

225 al. (2015) projections under the medium-high A1B scenario (Figure 3a; emulated median and
226 90% probability interval: 4.0 [3.7, 4.2] m; Ritz et al. (2015): 0.41 [0.04, 0.72] m) and more
227 than double the projections by Golledge et al. (2015)²⁸ for RCP8.5 (0.88 m and 1.52 m at
228 2200 for two model versions). Beyond 2200, the DP16-derived projections under RCP8.5
229 become increasingly inconsistent with Golledge et al. (2015) (Figure 3a); the 2.5th percentile
230 at 2500 without MICI is higher than the latter's projections at 2500 even under a doubling of
231 RCP8.5 temperature changes. This is particularly surprising, given DP16 greenhouse gas
232 concentrations are capped from the year 2175. However, the RCP4.5 and RCP2.6 No-MICI
233 projections are consistent: the Golledge et al. (2015) ranges fall within the 90% probability
234 intervals.

235 This suggests the DP16 model may be over-sensitive to very large atmospheric
236 temperature changes, even without MICI: i.e. the response is not self-limiting, due to
237 widespread ice shelf sensitivity to warming and/or a lack of local factors mitigating MISI
238 (e.g. bedrock topography, basal traction and sliding, theoretical constraints on ice stresses at
239 the grounding line, and predicted climatic triggers), in contrast to findings from a diversity of
240 other ice sheet and ice shelf models^{4,9,14,15,28,29}.

241

242 **Knowledge gaps and future directions**

243 Our analysis has two aims: to make best estimates of the probability distributions implied by
244 the DP16 study and satellite record, and to evaluate ways in which the original study could be
245 built upon to improve confidence in Antarctic projections. Altering the DP16 climate or ice
246 sheet models, and extending the ensemble parameter ranges, are beyond the scope of this
247 study. For example, we could test the effect of reducing the range of the ice cliff collapse
248 parameter VCLIF (Extended Data Figure 5), but not increasing it. These estimates therefore
249 incorporate many of the limitations of DP16, and should be seen as a first step towards a full
250 assessment of Antarctic sea-level uncertainty.

251 We made pragmatic, simple choices, such as using the same palaeodata intervals as
252 DP16 and uniform distributions for the parameters. Future work should explore alternatives:
253 sampling of the parameter space, palaeodata reconstructions with well-defined uncertainty
254 estimates, spatio-temporal patterns from satellite data, and Bayesian calibration. We are
255 confident that the tails of the sea-level distributions (essential to decision-making) have not
256 been truncated too much by the calibration, as we use a 99.7% probability interval for the
257 satellite data (see Methods) and the palaeodata have very little influence (Extended Data

258 Figure 5). Nevertheless we present projections only to the 95th percentile, to reflect our
259 judgement about the precision of these estimates. Most importantly, presence or absence of
260 MICI is by far the largest uncertainty in sea-level rise this century that could be quantified in
261 this study.

262 Although the maximum height of ice cliffs is founded in theory and indirectly
263 supported by observations and geological evidence^{18,30}, very little is known about whether
264 initial cliff collapse would lead to a positive feedback (i.e. MICI), how this would vary in
265 different locations, the consequent rate of ice wastage, and how long it would last. MICI
266 might be mitigated by cool, fresh meltwater entering the ocean, buttressing by ice mélange,
267 or changes in relative sea-level from gravitational and solid earth effects. Greenland's
268 Helheim and Jakobshavn glaciers have high rates of ice wastage, but this is dominated by
269 their fast flow, not grounding line retreat. Reducing the maximum ice wastage value by 20%
270 to 4 km/a reduces the RCP8.5 projected median by 14% and the 95th percentile by 17%
271 (Extended Data Figure 5), and higher maximum values (which it is not possible to explore in
272 this study) would likely have the opposite effect. The parameterisation of ice loss by MICI in
273 DP16 is very simple, and the low resolution of the model might also over-estimate the
274 occurrence of tall cliffs. A diversity of model parameterisations is therefore needed.

275 Triggers are also poorly understood. DP16 predict early and widespread surface melting
276 (DP16: Extended Data Figure 4) and ice shelf collapse, due to high atmospheric warming,
277 high sensitivity of melting/collapse to warming, or both. This is in contrast with studies using
278 process-based models, which predict up to 5-6 times less surface melting around the
279 Peninsula and 3-8 times less on the West Antarctic Abbot ice shelf by 2100 under RCP8.5¹⁰,
280 and that only shelves along the Peninsula are vulnerable this century under SRES A1B⁹ and
281 RCP8.5¹⁰. Observational evidence of ice shelf melting has highlighted both amplifying and
282 mitigating processes³¹⁻³³, and atmosphere and ocean models have limitations such as present
283 day biases and missing processes, so further process studies and monitoring are required. The
284 DP16 model shows low sensitivity to ocean melting (DP16 Figure 6) and apparently
285 unconstrained response to atmospheric warming (Figure 3a), in contrast with other
286 models^{4,9,14,15,28,29,34}. Again, a greater diversity of models is needed, along with standardised
287 extension of greenhouse gas concentration scenarios, in order to estimate ice sheet stability
288 on multi-centennial timescales. For the Pliocene, DP16 apply a 2°C ocean warming but
289 Golledge et al. (2017)³⁵ estimate this was 3°C, so the contribution to sea-level rise may be
290 under-estimated.

291 Using palaeo-reconstructions to calibrate models requires robust quantification of their
292 uncertainties. History matching calibrations typically use a mean \pm 3 s.d. interval, which for
293 continuous and unimodal distributions corresponds to 95% or greater probability³⁶ for
294 calibration with one observation. For the Pliocene, total GMSL change reconstructed by
295 Miller et al. (2012)³⁷ implies an Antarctic contribution of approximately 4-24 m (95% range),
296 Gasson et al. (2016)²⁰ estimated an Antarctic contribution of -1 to 13 m (with less confidence
297 in the lower bound), Golledge et al. (2017)³⁵ estimated an Antarctic contribution in the early
298 Pliocene of 3-14.2 m (95% range) – all equivalent to, or wider than, the interval used here
299 (i.e. no constraint) – while Raymo et al. (2018)³⁸ argue that Pliocene GMSL is effectively
300 unknown. For the LIG, we have assumed the DP16 range (3.5-7.4 m) is sufficiently broad,
301 but the GMSL estimate by Kopp et al. (2013)³⁹ implies a 90% interval for Antarctica of
302 around 1.6-7.5 m, while the 80% probability interval implied by Dusterhus et al. (2016)⁴⁰
303 (1.3-13.3 m) would virtually eliminate the LIG as a constraint. Long-term deformations in the
304 earth’s surface have also recently been estimated to potentially increase estimates of total
305 GMSL at the LIG by up to several metres⁴¹. In fact, emulated projections calibrated only with
306 the satellite period are virtually identical to those calibrated with all three eras (Extended
307 Data Figure 5), indicating that these evaluations with palaeodata have little impact. Using
308 Bayesian calibration (weighting ensemble members by their difference with the data) might
309 yield a stronger constraint, but this would require estimates of mean values and error
310 distributions (e.g. Gaussian).

311 The DP16 ensemble design is not optimal: it includes large gaps and effectively
312 duplicated simulations, and under-samples model uncertainties. Failing to incorporate model
313 error in the calibration also means their projections are likely too narrow and over-confident,
314 a problem amplified by sensitivity to the Pliocene lower bound. Ensemble designs should be
315 space-filling^{4,42} and test which uncertainties are most important to sample (e.g. ‘pre-
316 calibration’^{43,44}); emulation allows efficient ensemble design and sensitivity analysis.
317 Statistically-meaningful calibrations (such as history matching and Bayesian updating, with
318 model discrepancy) improves interpretation of the data constraints and robustness and
319 interpretation of the resulting projections.

320 Currently there are few probabilistic Antarctic model projections, and they assess
321 different uncertainties in different ways. We propose a new vision of a ‘grand ensemble’
322 designed across multiple diverse ice sheet models simultaneously, systematically sampling
323 parameters, structures, boundary conditions and initial conditions³⁴. Co-ordinated design
324 would allow multi-model emulation, a statistically rigorous method of interpreting and

325 combining different model projections, to estimate probability distributions that account for
326 multiple model structural uncertainties. The Ice Sheet Model Intercomparison Project
327 (ISMIP6) is bringing together an international consortium of ice sheet modellers to make
328 projections for the Greenland and Antarctic ice sheets⁴⁵; this presents an ideal opportunity to
329 design such a framework.

330

- 332 1. IPCC. *Working Group I Contribution to the IPCC Fifth Assessment Report*
333 *Climate Change 2013: The Physical Science Basis*. (Cambridge University
334 Press, 2013).
- 335 2. Little, C. M., Oppenheimer, M. & Urban, N. M. Upper bounds on twenty-first-
336 century Antarctic ice loss assessed using a probabilistic framework. *Nature*
337 *Climate Change* 3, 1–6 (2013).
- 338 3. Levermann, A. *et al.* Projecting Antarctic ice discharge using response functions
339 from SeaRISE ice-sheet models. *Earth Syst. Dynam.* 5, 271–293 (2014).
- 340 4. Ritz, C. *et al.* Potential sea-level rise from Antarctic ice-sheet instability
341 constrained by observations. *Nature* 528, 115–118 (2015).
- 342 5. Ruckert, K. L. *et al.* Assessing the Impact of Retreat Mechanisms in a Simple
343 Antarctic Ice Sheet Model Using Bayesian Calibration. *PLOS ONE* 12,
344 e0170052 (2016).
- 345 6. DeConto, R. M. & Pollard, D. Contribution of Antarctica to past and future sea-
346 level rise. *Nature* 531, 591–597 (2016).
- 347 7. Pollard, D., DeConto, R. M. & Alley, R. B. Potential Antarctic Ice Sheet retreat
348 driven by hydrofracturing and ice cliff failure. *Earth and Planetary Science*
349 *Letters* 412, 112–121 (2015).
- 350 8. Hellmer, H. H., Kauker, F., Timmermann, R., Determann, J. & Rae, J. Twenty-
351 first-century warming of a large Antarctic ice-shelf cavity by a redirected coastal
352 current. *Nature* 485, 225–228 (2012).
- 353 9. Kuipers Munneke, P., Ligtenberg, S. R. M., Van den Broeke, M. R. & Vaughan,
354 D. G. Firn air depletion as a precursor of Antarctic ice-shelf collapse. *Journal of*
355 *Glaciology* 60, 205–214 (2014).
- 356 10. Trusel, L.D. *et al.* Divergent trajectories of Antarctic surface melt under two
357 twenty-first-century climate scenarios. *Nature Geoscience*, 8(12), pp.927–932
358 (2015).
- 359 11. Vaughan, D. G. West Antarctic Ice Sheet collapse – the fall and rise of a
360 paradigm. *Climatic Change* 91, 65–79 (2008).
- 361 12. Schoof, C. Ice sheet grounding line dynamics: Steady states, stability, and
362 hysteresis. *Journal of Geophysical Research* 112, F03S28 (2007).
- 363 13. Rignot, E., Mouginot, J., Morlighem, M., Seroussi, H. & Scheuchl, B.
364 Widespread, rapid grounding line retreat of Pine Island, Thwaites, Smith, and
365 Kohler glaciers, West Antarctica, from 1992 to 2011. *Geophysical Research*
366 *Letters* 41, 3502–3509 (2014).
- 367 14. Favier, L. *et al.* Retreat of Pine Island Glacier controlled by marine ice-sheet
368 instability. *Nature Climate Change* 5, 117–121 (2014).
- 369 15. Joughin, I., Smith, B. E. & Medley, B. Marine Ice Sheet Collapse Potentially
370 Under Way for the Thwaites Glacier Basin, West Antarctica. *Science* 344, 735–
371 738 (2014).
- 372 16. Waugh, D. W., Primeau, F., DeVries, T. & Holzer, M. Recent Changes in the
373 Ventilation of the Southern Oceans. *Science* 339, 568–570 (2013).
- 374 17. Previdi, M. & Polvani, L. M. Climate system response to stratospheric ozone
375 depletion and recovery. *Q J Roy Meteor Soc* 140, 2401–2419 (2014).
- 376 18. Bassis, J. N. & Walker, C. C. Upper and lower limits on the stability of calving
377 glaciers from the yield strength envelope of ice. *Proceedings of the Royal Society*
378 *A: Mathematical, Physical and Engineering Sciences* 468, 913–931 (2012).
- 379 19. Sweeney, J., Salter-Townshend, M., Edwards, T., Buck, C. E. & Parnell, A. C.

- 380 Statistical Challenges in Estimating Past Climate Changes. *WIREs*
381 *Computational Statistics*, 10 (5), e1437 (2018).
382 <https://doi.org/10.1002/wics.1437>
- 383 20. Gasson, E., DeConto, R. M. & Pollard, D. Modeling the oxygen isotope
384 composition of the Antarctic ice sheet and its significance to Pliocene sea-level.
385 *Geology* 44, 827–830 (2016).
- 386 21. Williamson, D., Blaker, A., Hampton, C. & Salter, J. Identifying and removing
387 structural biases in climate models with history matching. *Climate Dynamics* 45,
388 1299–1324 (2014).
- 389 22. McNeall, D. *et al.* The impact of structural error on parameter constraint in a
390 climate model. *Earth Syst. Dynam.* 7, 917–935 (2016).
- 391 23. Williamson, D., Blaker, A. T. & Sinha, B. Tuning without over-tuning:
392 parametric uncertainty quantification for the NEMO ocean model. *Geosci. Model*
393 *Dev.* 10, 1789–1816 (2017). doi:10.5194/gmd-2016-185-AC3
- 394 24. Gladstone, R. M. *et al.* Calibrated prediction of Pine Island Glacier retreat during
395 the 21st and 22nd centuries with a coupled flowline model. *Earth and Planetary*
396 *Science Letters* 333-334, 191–199 (2012).
- 397 25. Shepherd, A. *et al.* Mass balance of the Antarctic Ice Sheet from 1992 to 2017.
398 *Nature* 558, 219–222 (2018).
- 399 26. Golledge, N., E. D. Keller, N. Gomez, K. A. Naughten, J. Bernales, L. D. Trusel,
400 and T. L. Edwards (2018), Causes and consequences of 21st century ice sheet
401 melt. *Submitted*.
- 402 27. Le Bars, D., Drijfhout, S. & de Vries, H. A high-end sea-level rise probabilistic
403 projection including rapid Antarctic ice sheet mass loss. *Environ Res Lett* 12,
404 044013 (2017).
- 405 28. Golledge, N. R. *et al.* The multi-millennial Antarctic commitment to future sea-
406 level rise. *Nature* 526, 421–425 (2015).
- 407 29. Cornford, S. L. *et al.* Century-scale simulations of the response of the West
408 Antarctic Ice Sheet to a warming climate. *The Cryosphere* 9, 1579–1600–
409 (2015).
- 410 30. Wise, M. G., Dowdeswell, J. A., Jakobsson, M. & Larter, R. D. Evidence of
411 marine ice-cliff instability in Pine Island Bay from iceberg-keel plough marks.
412 *Nature* 550, 506–510 (2017).
- 413 31. Bell, R. E. *et al.* Antarctic ice shelf potentially stabilized by export of meltwater
414 in surface river. *Nature* 544, 344–348 (2017).
- 415 32. Kingslake, J., Ely, J. C., Das, I. & Bell, R. E. Widespread movement of
416 meltwater onto and across Antarctic ice shelves. *Nature* 544, 349–352 (2017).
- 417 33. Gourmelen, N. *et al.* Channelized Melting Drives Thinning Under a Rapidly
418 Melting Antarctic Ice Shelf. *Geophysical Research Letters* 17, 173 (2017).
- 419 34. Pattyn, F., Favier, L., Sun, S. & Durand, G. Progress in Numerical Modeling of
420 Antarctic Ice-Sheet Dynamics. *Curr Clim Change Rep* 3, 174–184 (2017).
- 421 35. Golledge *et al.* (2017), Antarctic climate and ice-sheet configuration during the
422 early Pliocene interglacial at 4.23 Ma, *Climate of the Past*, 13(7), pp.959–975.
- 423 36. Pukelsheim, F. The three sigma rule. *The American Statistician* 48, 88–91
424 (1994).
- 425 37. Miller, K. G. *et al.* High tide of the warm Pliocene: Implications of global sea-
426 level for Antarctic deglaciation. *Geology* 40, 407–410 (2012).
- 427 38. Raymo, M.E. *et al.*, 2018. The accuracy of mid-Pliocene $\delta^{18}\text{O}$ -based ice volume
428 and sea level reconstructions. *Earth-Science Reviews*, 177, pp.291–302.
- 429 39. Kopp, R. E., Simons, F. J., Mitrovica, J. X., Maloof, A. C. & Oppenheimer, M.

- 430 A probabilistic assessment of sea-level variations within the last interglacial
431 stage. *Geophysical Journal International* 193, 711–716 (2013).
- 432 40. Düsterhus, André, Tamisiea, M. E. & Jevrejeva, S. Estimating the sea-level
433 highstand during the Last Interglacial: a probabilistic massive ensemble
434 approach. *Geophysical Journal International* 206, 900–920 (2016).
- 435 41. Austermann, J., Mitrovica, J. X., Huybers, P. & Rovere, A. Detection of a
436 dynamic topography signal in last interglacial sea-level records. *Science*
437 *Advances* 3, 1–9 (2017).
- 438 42. Nias, I., Cornford, S. L. & Payne, A. J. Contrasting model sensitivity of the
439 Amundsen Sea embayment ice streams. *Journal of Glaciology* 62, 552–562
440 (2016).
- 441 43. Holden, P. B., Edwards, N. R., Oliver, K. I. C., Lenton, T. M. & Wilkinson, R.
442 D. A probabilistic calibration of climate sensitivity and terrestrial carbon change
443 in GENIE-1. *Climate Dynamics* 35, 785–806 (2009).
- 444 44. Edwards, N. R., Cameron, D. & Rougier, J. Precalibrating an intermediate
445 complexity climate model. *Climate Dynamics* 37, 1469–1482 (2011).
- 446 45. Nowicki, S. M. J. *et al.* Ice Sheet Model Intercomparison Project (ISMIP6)
447 contribution to CMIP6. *Geosci. Model Dev. Discuss.* 1–42 (2016).
448 doi:10.5194/gmd-2016-105-SC2
449

450 **Acknowledgements**

451 T.L.E., N.E. and P.H. were supported by EPSRC REsearch on Changes of Variability and
452 Environmental Risk (ReCoVER: EP/M008495/1) under the Quantifying Uncertainty in
453 ANTarctic Ice Sheet instability (QUAntIS) project (RFFLP 006). T.L.E. was also supported
454 by the EPSRC-funded Past Earth Network (EP/M008363/1) and the Université Joseph
455 Fourier – Grenoble International visitor fund ‘Campagne INVITES’. N.R.G is supported by
456 contract VUW1501 from the Royal Society Te Aparangi. I.N. was supported by the NERC
457 iSTAR-C project Dynamical control on the response of Pine Island Glacier (NE/J005738/1)
458 and now by the NASA Sea Level Change program. A.W. is supported by the Open
459 University Faculty of Science, Technology, Engineering and Mathematics.

460 Thanks to Rob DeConto for running additional simulations necessary for the analysis,
461 suggestions and helpful discussions, and to Kelsey Ruckert and Anders Levermann for
462 providing data. Thanks to the statisticians who attended the Past Earth Network events
463 ‘Assessing Palaeoclimate Uncertainty’ (held jointly with the Environmental Statistics Section
464 of the Royal Statistics Society, Cambridge, August 2016), ‘Emulators workshop’ (Leeds,
465 June 2017), and writing retreat (Callow Hall, August 2017) for their advice, particularly Ian
466 Vernon, Peter Challenor, and Jonty Rougier. Thanks to Dewi Le Bars, Doug McNeill, David
467 Demeritt and the King’s Geography Hazards, Risk and Regulation reading group (George
468 Adamson, Felicia Liu, Amar Razli, Laurence Ball and Ana Heilbron) for helpful comments
469 on the manuscript. Thanks to three anonymous reviewers for their comments and advice.

470 Thanks also to Dr Kai-Keen Shiu of UCL Hospitals for supporting this work, and to Dallas
 471 Campbell for everything.

472

473 **Author contributions**

474 T.L.E. conceived the idea, carried out the analysis, produced the figures, and wrote the
 475 manuscript. A.W. and P.B.H. performed preliminary analyses. A.J.P, A.W., C.R., G.D., I.N.,
 476 M.B. and N.R.G. contributed ideas on glaciological and oceanic aspects, while A.W., N.R.E.
 477 and P.B.H. contributed ideas on statistical aspects. All authors contributed to writing the
 478 manuscript.

479

480 **Author information**

481 The authors declare no competing financial interests. Correspondence and requests for
 482 materials should be addressed to T.L.E. (tamsin.edwards@kcl.ac.uk).

483

484 **Table 1. Probabilities from DeConto and Pollard (2016) study.** Means and standard deviations, and implied
 485 probability intervals, for DeConto and Pollard (2016) ensemble at 2100 for RCP8.5 for their four
 486 methodological choices (see text), using minimal assumptions about the distribution shape (finite mean and
 487 variance: Chebyshev inequality).

RCP8.5	LOW PLIOCENE		HIGH PLIOCENE	
	Bias	Bias	Bias	Bias
	Uncorrected	Corrected	Uncorrected	Corrected
Antarctic contribution at 2100 (cm sea-level equivalent)				
Mean \pm 1 s.d.	64 \pm 49	79 \pm 46	105 \pm 30	114 \pm 36
\geq 68% probability interval	[-22, 150]	[-2, 160]	[51, 158]	[51, 177]
\geq 90% probability interval	[-90, 217]	[-65, 223]	[9, 200]	[1, 227]

488

489

490 **Table 2. Projections for the Antarctic contribution to sea-level in 2100.** Calibrated with Pliocene, Last
 491 Interglacial and satellite data (1997-2017), with and without DeConto and Pollard (2016) marine ice cliff
 492 instability (MICI) parameterisation.

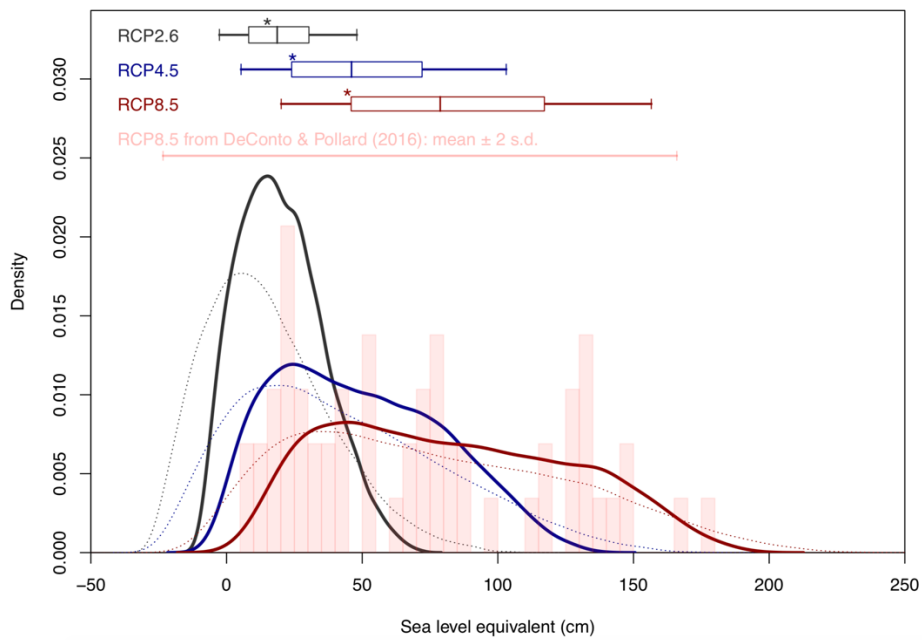
493

	RCP2.6		RCP4.5		RCP8.5	
	No MICI	MICI	No MICI	MICI	No MICI	MICI
Antarctic contribution at 2100 (cm sea-level equivalent)						
Mode	-6	15	0	24	15	45
Median	-1	19	5	46	21	79
Mean	0	20	7	49	22	83
68% interval	[-7, 8]	[4, 36]	[-1, 15]	[16, 83]	[13, 32]	[35, 133]
90% interval	[-9, 13]	[-3, 48]	[-3, 21]	[5, 103]	[9, 39]	[20, 157]
Exceedance probabilities						
≥ 30 cm	--	26%	--	68%	20%	88%
≥ 50 cm	--	4%	--	46%	--	71%
≥ 1 m	--	--	--	6%	--	36%

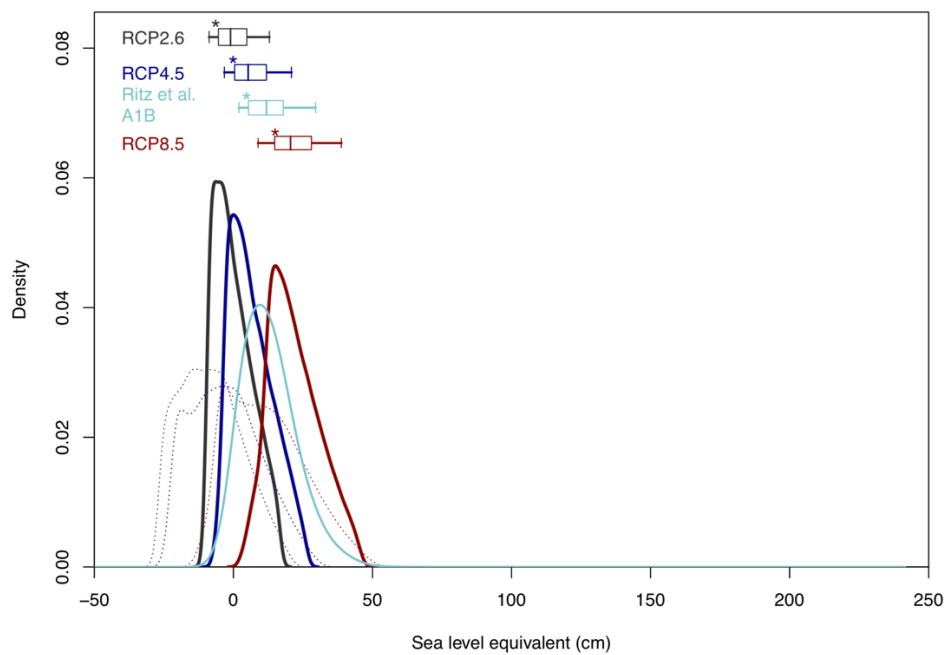
494

495

496



497



498

499

500

501

502

503

504

505

506

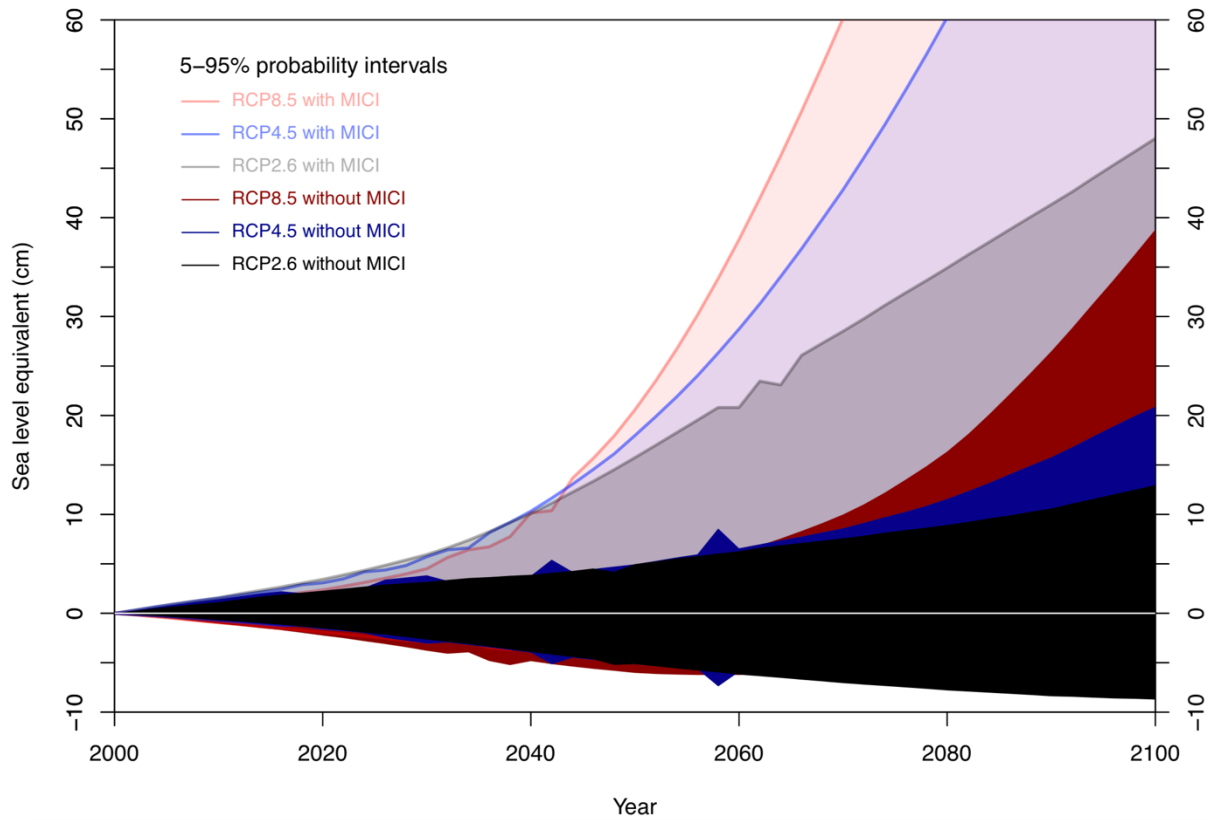
507

508

Figure 1. Probabilistic projections of the Antarctic contribution to sea-level at 2100. Projections estimated under three RCPs, (a) with ice cliff instability parameterisation and (b) without, from emulation of the DeConto and Pollard (2016) ice sheet model ensemble. Dotted lines are the uncalibrated emulator ensemble; solid lines are calibrated with Last Interglacial and Pliocene reconstructions and satellite data from 1992-2017. Box and whiskers show the [5, 25, 50, 75, 95]th percentiles; star shows the mode. The DeConto and Pollard (2016) ensemble members for RCP8.5 (LowPliocene calibration; BiasCorrected and BiasUncorrected combined) are shown as a histogram and mean \pm 2 s.d. interval in (a). The projection for the Antarctic contribution due to ice discharge under the medium-high climate scenario A1B by Ritz et al. (2015) is also shown in (b). Data from refs. 6 and 25 and supplementary simulations by R. DeConto (pers. comm.) (see Methods).

509

510



511

512

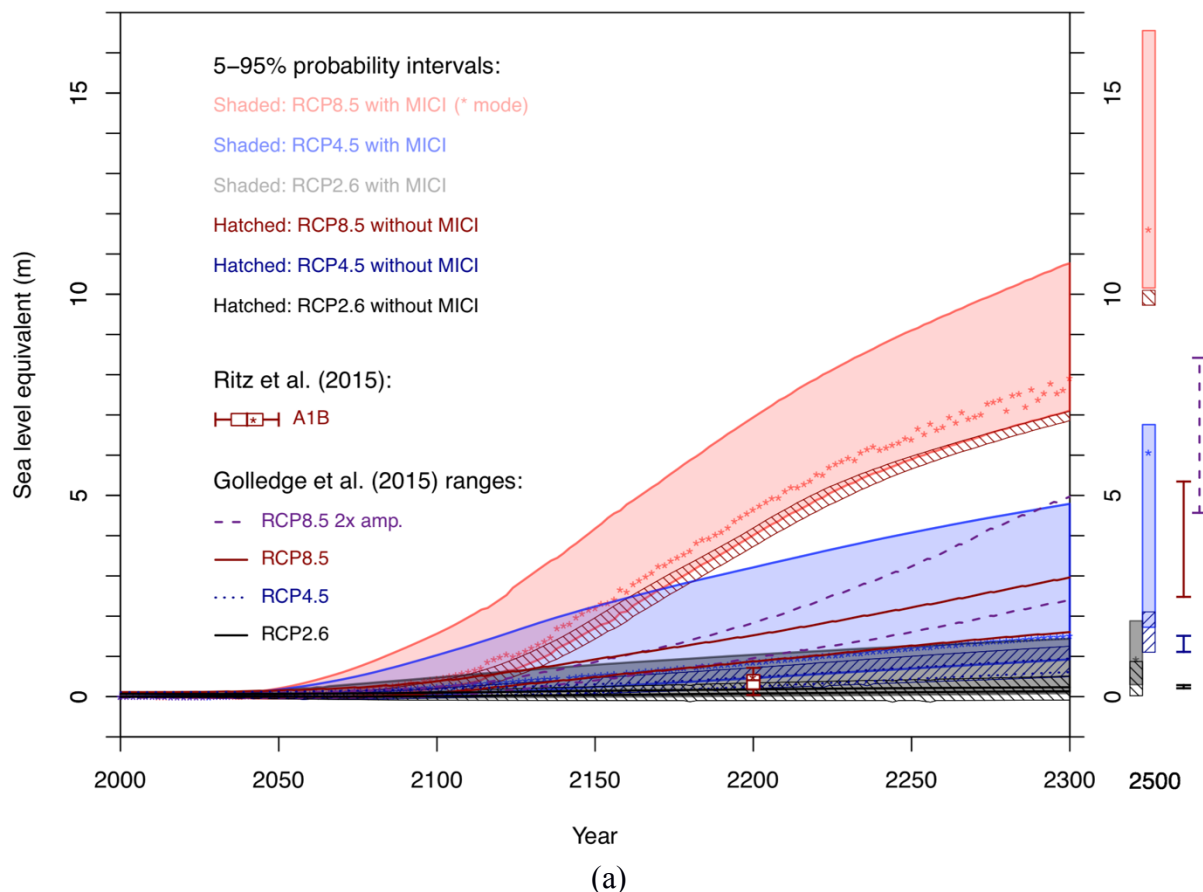
513

514

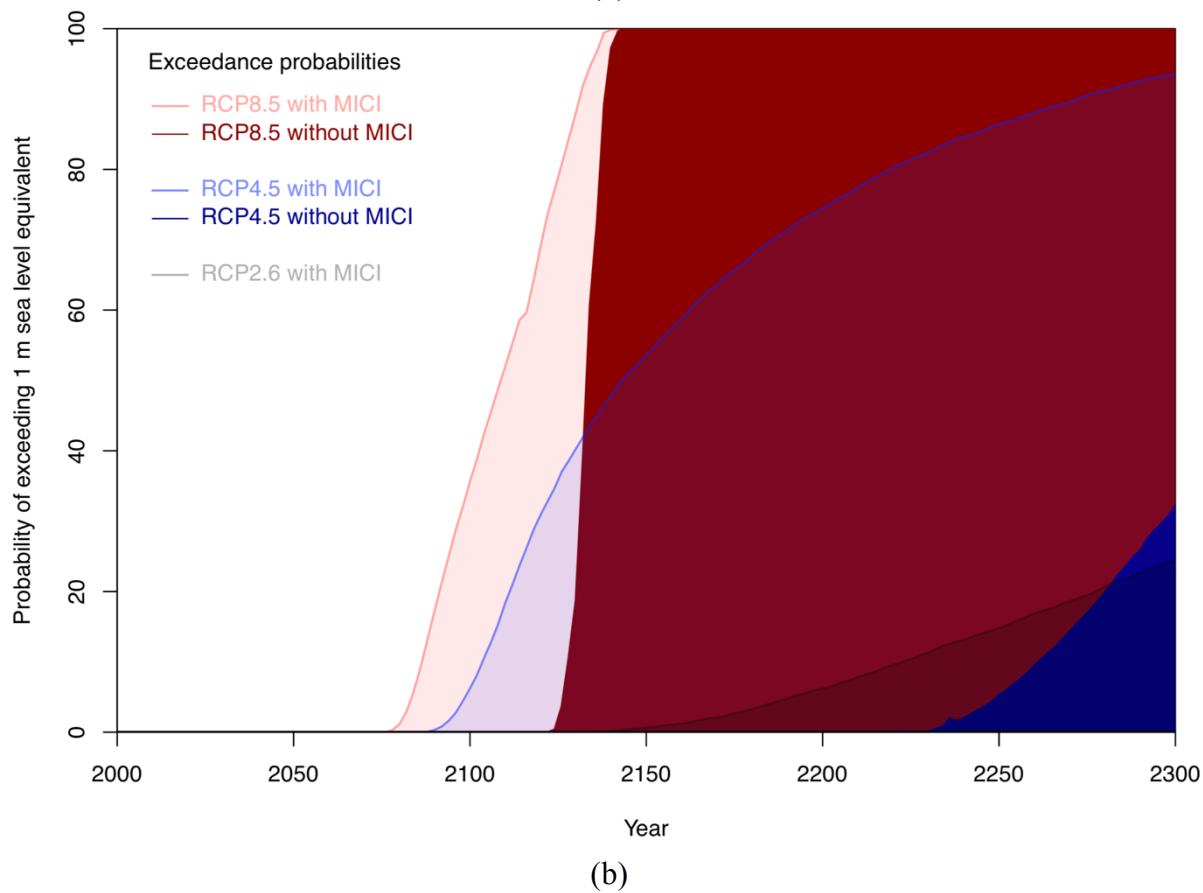
515

516

Figure 2. Emergence of ice cliff instability. Projected 5-95% probability intervals for Antarctic sea-level contributions this century, with and without the marine ice cliff instability (MICI) parameterisation of DeConto and Pollard (2016). Data from refs. 6 and 25 and supplementary simulations by R. DeConto (pers. comm.) (see Methods).



517
518



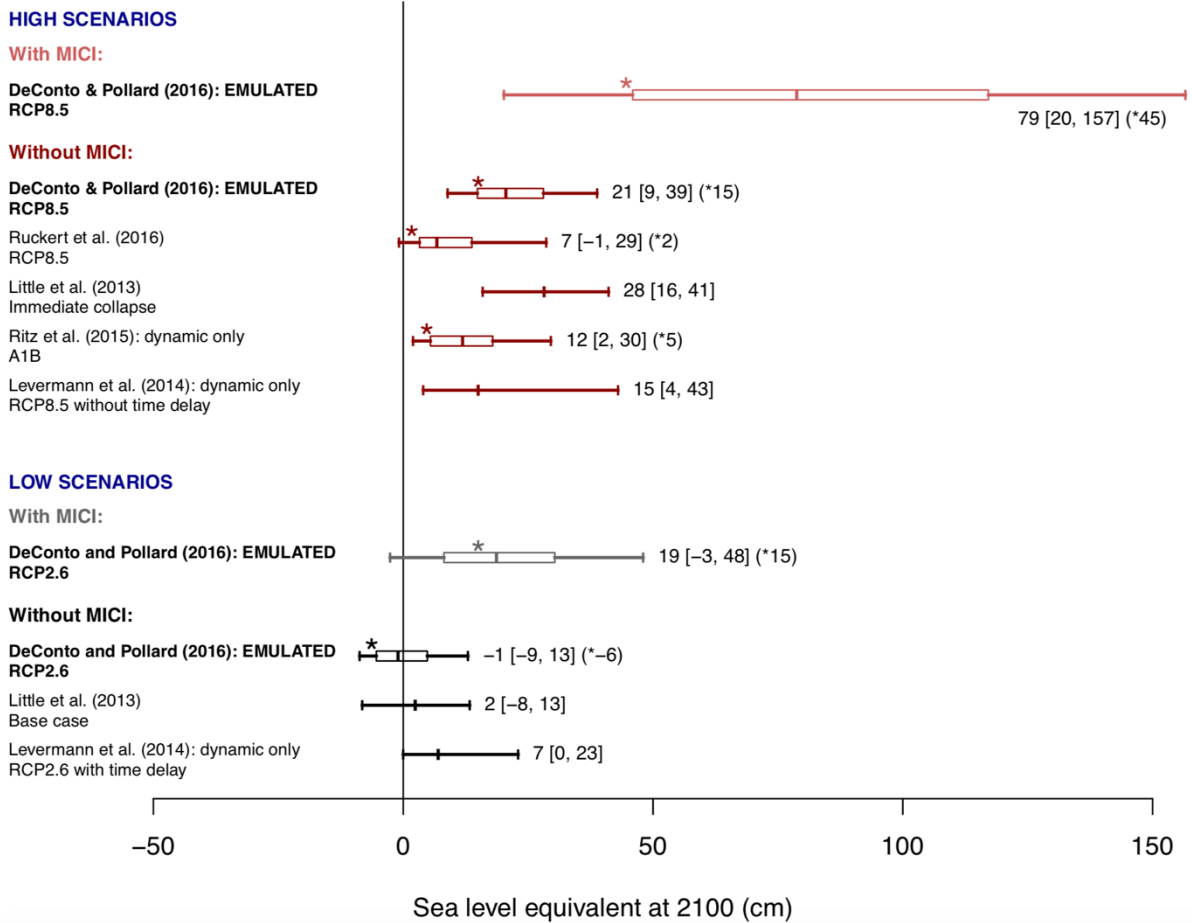
519
520

521 **Figure 3. Long-term projections of Antarctic sea-level contribution.** (a) Shaded/hatched regions: projected
522 5-95% intervals for Antarctic sea-level contribution to 2300 and for 2500 with (shaded) and without (hatched)
523 ice cliff instability (MICI) parameterisation under three greenhouse gas concentration scenarios. Dots: mode of
524 the RCP4.5 and RCP8.5 distributions with MICI. Single lines: range of results from Golledge et al. (2015) under
525 RCP8.5 (solid dark red), RCP8.5 with doubled atmosphere and ocean temperature changes (dashed purple),
526 RCP4.5 and RCP2.6 (solid black). Box and whisker at 2200 shows Ritz et al. (2015): [5, 25, 50, 75, 95]th
527 percentiles and mode (*). (b). Projected probability of exceeding 1 m Antarctic sea-level contribution over the
528 same period. Data from refs. 6 and 25 and supplementary simulations by R. DeConto (pers. comm.) (see
529 Methods).

530

531

532



534

535

536

537

538

539

540

541

542

543

544

545

546

547

548

Figure 4. Multi-model comparison. Projections from this study (bold text: ‘EMULATED’) at 2100 based on emulation of DeConto and Pollard (2016) (with and without ice cliff instability, ‘MICI’), along with results from other probabilistic modelling studies. Box and whiskers show the [5, 25, 50, 75, 95]th percentiles; star shows the mode. Numbers show the median, [5th, 95th] percentiles and, where available, the mode (*). “High Scenarios” (pink/red) are for high-end (RCP8.5) or medium-high (Special Report on Emissions Scenario A1B¹) greenhouse gas emissions or concentrations, or immediate collapse of part of West Antarctica (Little et al. (2013): 5th percentile and median are estimated from digitisation); Levermann et al. (2014) is from models with ice shelves, without time delay. “Low Scenarios” (grey/black) are for low greenhouse gas concentrations (RCP2.6) or other baseline case (Little et al., 2013); Levermann et al. (2014) is with time delay. Levermann et al. (2014) and Ritz et al. (2015) are for ice discharge contribution only. Data from refs. 2-6 and 25, supplementary simulations by R. DeConto (pers. comm.), and mode for ref. 5 supplied by K.L. Ruckert (pers. comm) (see Methods).

549 **METHODS**

550 **Simulator ensemble design**

551 DeConto and Pollard (2016) perturb three continuous parameters, sampling four levels for
552 each in a factorial design to generate $4^3 = 64$ ensemble members:

553 **OCFAC**: Ocean melt factor, which controls sub-ice-shelf direct melting. Defined as a
554 factor by which the default value is multiplied. $\text{OCFAC} = \{0.1, 1, 3 \text{ and } 10\} \times 0.224 \text{ m yr}^{-2}$
555 $^{\circ}\text{C}^{-2}$.

556 **CREVLIQ**: Crevasse liquid depth, which controls ice shelf collapse by hydrofracturing
557 due to surface liquid. Defined as the additional crevasse depth due to surface melt plus
558 rainfall rate. $\text{CREVLIQ} = \{0, 50, 100, 150\} \text{ m per } (\text{m yr}^{-1})^{-2}$.

559 **VCLIF**: Maximum net ice wastage rate. Controls cliff failure after ice shelf collapse.
560 $\text{VCLIF} = \{0, 1, 3, 5\} \text{ km yr}^{-1}$.

561 When emulating the ice sheet model (see below) we treat ocean bias correction as an
562 continuous uncertain parameter:

563 **BIAS**: Southern Ocean bias correction applied to present day and future simulations.
564 Defined as a scalar ranging from 0 (no bias correction, $+0^{\circ}\text{C}$) to 1 (full bias correction,
565 $+3^{\circ}\text{C}$). Active only for present day and future simulations.

566 We use time series data for the ensemble provided by Rob DeConto. When emulating
567 the model, we found a sign error in the DP16 Supplementary Information: the Last
568 Interglacial value for simulation row 6 ($\text{OCFAC} = 0.1$, $\text{CREVLIQ} = 50$, $\text{VCLIF} = 1$) should
569 be $+2.63 \text{ m}$, not -2.63 m .

570

571 **Building the emulators**

572 We use Gaussian Process regression ('kriging' when used for spatial interpolation), because
573 it is flexible, non-parametric, and provides uncertainty estimates⁴⁶. As usual for emulation of
574 computer models, we set the 'nugget' to zero because the ice sheet model is deterministic.
575 We refer to 'the emulator' in the main text for simplicity, but this comprises separate
576 emulators for each scalar output: Pliocene and LIG sea-level change, present day (1992-2017
577 change in the RCP4.5 simulation) and the change from 2000 to every even-numbered year up
578 to 2500 for the three RCPs. We construct, validate, calibrate and make predictions using the
579 R software packages DiceKriging and a modified version of DiceEvaluation.

580 Let the function $f(x)$ be the ice sheet model, which simulates sea-level change in a
581 particular era (e.g. the Pliocene) as a function of the set of its input parameters, x . We

582 consider only one output at a time, to avoid the need for a further index. An emulator $f_{em}(x)$
 583 for a particular output of $f(x)$ can be written as:

$$f_{em}(x) = \sum_j \beta_j g_j(x) + u(x)$$

584
 585 where $g(x)$ are known functions of x , β are regression coefficients, and $u(x)$ is a stochastic
 586 process with a specified covariance function. We wish to select the subset of x that has the
 587 most influence on $f_{em}(x)$.

588 Design and validation of the emulators comprises two parts: a step-wise model
 589 selection procedure, to choose the mean function (i.e. which simulator parameters, and
 590 interactions between these, to use as regressors), and a ‘leave-one-out’ (LOO) cross-
 591 validation procedure, to evaluate which is the most suitable covariance function and whether
 592 each emulator is sufficiently accurate for our purposes. We perform these procedures for six
 593 outputs — the two palaeo-eras, the present day, and the three RCP projections at 2100 — to
 594 choose the overall emulator structure. The final fitting of the emulators with the full ensemble
 595 data, and their use for prediction, are discussed later.

596

597 *Mean functions:* There are important interactions between parameters — for example,
 598 increasing the bias correction (BIAS) increases the effect of maximum ice wastage rate
 599 (VCLIF) on projections — but we also wish to avoid over-fitting by including too many
 600 interaction terms. We use the R MASS package’s stepAIC to select model terms, testing up
 601 to second order (three-way) interactions between parameters, using Bayesian Information
 602 Criterion because it is generally more parsimonious than Akaike Information Criterion. The
 603 resulting mean functions for the six outputs are:

604

605 Pliocene and Last Interglacial:

606 $g_{\text{palaeo}}(x) \sim (\text{OCFAC}, \text{CREVLIQ}, \text{VCLIF}, \text{CREVLIQ}*\text{VCLIF})$

607

608 Present day and RCP2.6 at 2100:

609 $g_{\text{low}}(x) \sim (\text{OCFAC}, \text{CREVLIQ}, \text{VCLIF}, \text{BIAS}, \text{OCFAC}*\text{VCLIF}, \text{OCFAC}*\text{BIAS},$
 610 $\text{CREVLIQ}*\text{VCLIF}, \text{VCLIF}*\text{BIAS}, \text{OCFAC}*\text{VCLIF}*\text{BIAS})$

611

612 RCP4.5 and RCP8.5 at 2100:

613 $g_{\text{high}}(x) \sim (\text{OCFAC}, \text{CREVLIQ}, \text{VCLIF}, \text{BIAS}, \text{OCFAC}*\text{VCLIF}, \text{OCFAC}*\text{BIAS},$
 614 $\text{CREVLIQ}*\text{VCLIF})$

615

616 where $g \sim (a,b)$ means g is a linear function of a and b , etc, and $a*b$ indicates an interaction
617 term.

618

619 *Covariance functions:* The covariance controls the smoothness between data points, with a
620 trade-off between accuracy and over-fitting. We compare the success of different covariance
621 functions — Matern(5/2), Matern(3/2), exponential, and power-exponential (exponential
622 family, where the exponent can vary between 0 and 2) — using the mean function selected
623 above, and choose the one with the smallest normalised Euclidean distance in a LOO
624 procedure. The LOO procedure comprises fitting the emulator to all ensemble members
625 except one (63 of 64), and then predicting the final member to compare with the simulation
626 itself. This is repeated for all 64 combinations to provide a summary statistic. Normalised
627 Euclidean distance is:

$$d = \sqrt{\sum_{i=1}^{64} \frac{(f_{em}(x_i) - f(x_i))^2}{\sigma_{em:x_i}^2}}$$

628

629 where i is the ensemble member and σ_{em} is the emulator error for that prediction. We choose
630 this metric because it makes use of the uncertainty estimate inherent in a Gaussian Process
631 emulator to standardise the residuals, so that an emulator with some large errors is not overly
632 penalised if it has sufficiently large uncertainty estimates to generally encompass the true
633 value. This also guards against overfitting, by penalising too-confident emulators. The
634 distance metric therefore balances the two aims of emulator accuracy and appropriate
635 confidence. The resulting covariance functions from this procedure are power-exponential for
636 the LIG, Matern(3/2) for 1992-2017, and exponential for the Pliocene and future outputs.

637

638 **Validating and fitting the emulators**

639 We use various validation outputs to assess emulator adequacy: RMSE; Kendall's tau, a non-
640 parametric measure of correlation, for the emulator predictions versus the simulations; and
641 the fraction of predictions for which the simulation lies within the emulator 95% credibility
642 interval, for which values lower than ~90% would indicate an over-confident emulator (i.e.
643 too-small uncertainty estimates). The RMSE and Kendall rank correlation coefficients
644 between the emulator predictions and simulations are 12 cm (1.4% of the data range) and
645 0.958 respectively for the Pliocene; 26 cm (2.7%) and 0.923 for the Last Interglacial; 0.1 cm
646 (0.6%) and 0.972 for the present day, and 0.9-1.2 cm (0.4-0.8%) and 0.973-0.976 for the

647 three future projection emulators, indicating sufficient accuracy. The fraction of predictions
648 within the emulator 95% interval is 100% for the Pliocene, 89% for the LIG, and 91-98% for
649 the present and future, indicating sufficiently large emulator uncertainty estimates. The
650 predictive accuracy and uncertainty estimates of the six emulators can also be inspected
651 visually by plotting the emulator predictions vs simulations and the standardised residuals
652 (Extended Data Figure 6).

653 Having judged these six emulators to be adequate, we fit each emulator with the full 64-
654 member ensemble for that output. We use the emulator structures for the year 2100 for all
655 timeslices for that RCP.

656

657 **Emulator ensemble design**

658 We predict 10,000 points in the parameter space using a maximin Latin Hypercube (i.e.
659 efficiently space-filling) design. The MICI design samples from uniform distributions for all
660 four parameters, based on discussion with one of the original DP16 authors (DeConto, pers.
661 comm.); the No-MICI design has VCLIF set to zero. The effect of VCLIF, CREVLIQ and
662 OCFAC on sea-level contribution at 2100 under RCP8.5 in the MICI case is shown in
663 Extended Data Figure 7, which shows the strong dependence on VCLIF. The reason for some
664 apparent gaps in emulator coverage is that the ensemble design is space-filling but does not
665 necessarily sample points in each corner of the parameter space, as the original ensemble
666 members do.

667

668 **Pliocene calibration**

669 The LowPliocene and HighPliocene projections of DP16 are presented (and have been
670 interpreted by others^{27,47}) as equally plausible, but here we make the case that the
671 HighPliocene calibration is not robust. This is important because the RCP8.5 projections are
672 uniquely sensitive to the particular minimum value chosen for the HighPliocene constraint
673 (10 m). Extended Data Figure 2a and b show that when the lower bound exceeds 9.6 m, this
674 results in much higher means and much smaller standard deviations, because fewer than a
675 quarter of the ensemble members pass. The sensitivity is caused by a combination of the
676 small ensemble size and the strong correlation in the model between Pliocene sea-level and
677 RCP8.5 projections (large circles in Extended Data Figure 3a).

678 This sensitivity to the Pliocene lower bound is exacerbated by the choice of calibration
679 method: a simple ‘accept’ or ‘reject’, which can be expressed in the ‘history matching’
680 framework^{22,48} below. This binary filtering means we should choose a sufficiently wide range

681 of tolerance, because every rejected ensemble member is treated as completely implausible
682 (by being removed, rather than down-weighted as in Bayesian calibration). Treating two
683 ranges as equally plausible is not coherent, because it implies values in the range 5–10 m and
684 15-20 m are simultaneously both plausible and implausible. The chosen data range should be
685 both broad and unique to obtain a calibration that is robust and meaningful.

686 Gasson, DeConto and Pollard (2016)²⁰ estimate the Antarctic contribution to mid-
687 Pliocene sea-level has a maximum of 13 m, which would rule out most of the HighPliocene
688 range, suggesting the interval 10-20 m is not well supported. (A range of 10-13 m would be
689 inconsistent with the large degree of uncertainty in Pliocene reconstructions^{37,49})

690 In fact, increasing the upper bound from 13 m would have no effect, because the
691 maximum Pliocene change in the ensemble is 12.4 m. Decreasing the lower bound below 5 m
692 would also make little difference, because the original (no discrepancy) DP16 Last
693 Interglacial calibration (3.5-7.4 m) rejects these ensemble members: none of the ensemble
694 members that pass the LIG constraint have Pliocene sea-level changes of less than 5 m
695 (Extended Data Figure 4: no large circles directly below shaded box). The crucial judgement
696 is therefore whether the 10 m HighPliocene lower bound can be justified.

697 We conclude that Pliocene Antarctic sea-level contribution is currently too uncertain to
698 use the HighPliocene constraint, particularly for this model and for a history matching
699 approach, and that the LowPliocene calibration is far more robust.

700

701 **Model discrepancy**

702 Model ‘discrepancy’, or ‘structural error’, is defined as the smallest possible difference
703 between a model simulation and the true values: that is, how well the model could reproduce
704 reality at its best possible, ‘tuned’, parameter values^{4,21,22,23}. Discrepancy is an essential part
705 of model calibration: not incorporating it implies that a model could be tuned to perfectly
706 match reality. Using a value less than the observational error would imply we could simulate
707 reality better than we could measure it. Model discrepancy can, in some cases, be
708 approximately estimated by comparing simulations with multiple observations. But if there
709 are insufficient observations to do this, as is the case here, discrepancy can be viewed as a
710 tolerance to model error⁴⁸ estimated by expert judgement^{4,24} (see below).

711

712 **Calibrating projections**

713 We re-express the DP16 calibration within a history matching framework, extending it to
714 account for emulator error and model discrepancy. We adapt notation by Vernon et al.

715 (2010)⁵⁰ here. The relationship between a palaeodata reconstruction or an observation of sea-
 716 level change (Pliocene, LIG, or 1992-2017 trend), z , and the true value, y , is modelled as:

$$717 \quad z = y + \epsilon_{obs}$$

718 where ϵ_{obs} has variance σ_{obs}^2 , the square of the observational or palaeodata reconstruction
 719 error. The relationship between the true value and the simulation of this sea-level change is:

$$720 \quad y = f(x^*) + \epsilon_{md}$$

721 where x^* are the best values of the parameters, and ϵ_{md} is the model discrepancy with
 722 variance σ_{md}^2 . We emulate $f(x)$:

$$723 \quad f(x) = f_{em}(x) + \epsilon_{em:x}$$

724
 725 where $f_{em}(x)$ is the mean emulator prediction for $f(x)$, and $\epsilon_{em:x}$ is the emulator error as
 726 before; it varies with x , and is automatically estimated in Gaussian Process emulation. For a
 727 given emulated output (Pliocene, LIG, 1992-2017 trend) we can use the standardised
 728 distance, also known as *implausibility*, I :

$$729 \quad \mathcal{I}^2(x) = \frac{(f_{em}(x) - z)^2}{\sigma_{obs}^2 + \sigma_{em:x}^2 + \sigma_{md}^2}$$

730 to accept or reject a given emulated ensemble member with parameter values x . We interpret
 731 the accepted ensemble members as a posterior probability distribution. This represents a
 732 judgement that this distribution represents our uncertainty about future sea-level rise (given
 733 the limitations of the ice sheet model and palaeodata), i.e. that the parameter space outside the
 734 calibration intervals has a low probability of being plausible.

735 We use a minimum LIG palaeodata value of 3.5 m, rather than the 3.6 m quoted by
 736 DP16, for consistency with their calibrated ensemble results which include a member with
 737 LIG sea-level change of 3.53 m.

738 The palaeodata reconstruction errors are not defined. We conservatively treat the
 739 DP16 range as a mean \pm 1 s.d. interval, so use $\sigma_{obs} = \{5, 2\}$ m for the Pliocene and LIG
 740 respectively. The observational constraint (Shepherd et al., 2018)²⁵ is the cumulative mass
 741 loss from 1992-2017, (2720 ± 1390) Gt, converted to cm sea-level equivalent by dividing by

742 3600, to give (0.756 ± 0.386) cm sea-level contribution over this period. Model discrepancy
743 is set to $\sigma_{md} = 0.5$ cm for 1992-2017 sea-level change.

744 When calibrating with palaeodata, we accept ensemble members with $I < 1$ for the
745 Pliocene and LIG, so that the simplest case without emulator and model errors matches the
746 interval used by DP16. We note this Pliocene range approximately corresponds to a 95%
747 interval in some reconstructions, but the LIG range may correspond to a lower probability
748 than 95% by some estimates, and so may be too strict a constraint (see main text). Calibration
749 with satellite data observations accepts ensemble members with $I < 3$, to follow the usual
750 history matching convention for well-defined errors: for a smooth unimodal distribution, $I <$
751 3 with probability greater than or equal to 95% (Pukelsheim, 1994)³⁶; for Gaussian
752 distributions, as we expect for the satellite data errors, the probability interval is 99.7%.

753 Extended Data Figure 3 shows the ‘calibration relationships’ for RCP8.5 at 2100: the
754 relationships between past and future. Grey boxes show the original palaeodata constraints;
755 dashed lines show the broader intervals after accounting for model discrepancy. Accounting
756 for emulator error in the implausibility means that some emulator ensemble members are
757 accepted that lie just outside the calibration interval.

758 Percentiles and exceedance probabilities are estimated directly from the 10,000-
759 member emulator ensemble, and modes from kernel density estimation using an automatic
760 (Silverman) bandwidth. We do not include emulator uncertainties in the distributions; these
761 are small at 2100, but increase on multi-century timescales so would broaden these
762 distributions. To improve the clarity of Figure 3, we exclude 1, 3 and 5 data points from each
763 of RCP8.5, RCP4.5 and RCP2.6 MICI projections respectively, because the estimates are not
764 continuous in time (due to slight differences in emulator fitting).

765

766 **Multi-model comparisons**

767 We show distributions from Ruckert et al. (2016)⁵ provided by Kelsey Ruckert, and estimate
768 the distribution at 2100 for Little et al. (2013)² by digitisation of the original figures. We re-
769 estimate the modes for Ritz et al. (2015)⁴ distributions using an automatic bandwidth for the
770 kernel density estimation, rather than the broader, fixed bandwidth used in the original study.
771 We assume differences due to definitions of time period are small enough to be ignored: all
772 are 2000-2100, except Little et al. (2013)² (1990-2099) and the IPCC¹ (1986–2005 to 2081–
773 2100 for Antarctic component).

774

775 **Palaeodata uncertainties**

776 We here consider probability intervals for palaeodata constraints. Peak total sea-level change
777 for the LIG estimated by Kopp et al. (2013)³⁹ is 6.4-10.9 m (90% probability interval), and by
778 Dusterhus et al. (2016)⁴⁰ is 6.1-16.7m (80% probability). These broadly encompass recent
779 assessments that the upper end of the widely used 6-9 m range⁴⁹ could increase by several
780 metres⁴¹. Subtracting a range of estimates for the contributions from Greenland, thermal
781 expansion and glaciers in the same way as Ruckert et al. (2016)⁵ (3.4-4.8 m) gives Antarctic
782 contributions of 1.6-7.5 m and 1.3-13.3 m respectively.

783 For the Pliocene, Miller et al. (2012)³⁷ estimate 22 ± 10 m (95% range) total sea-level
784 change; subtracting 7 m for the Greenland ice sheet and 1 m for thermal expansion (Golledge
785 et al., 2017)³⁵ would imply approximately 14 ± 10 m Antarctic contribution, i.e. 4-24 m.
786 There is no difference between using a combined 5-25 m range and using the LowPliocene
787 (5-15 m) constraint presented here, because the DP16 ensemble maximum is 12.4 m, though
788 for a different model or ensemble design the upper bound might have more influence.
789 Golledge et al. (2017)³⁵ estimate 8.6 ± 2.8 m for the Antarctic contribution to the early
790 Pliocene, and we use their Gaussian assumption to derive the 95% (2σ) range.

791

792 **Code availability**

793 All emulation was performed in R using the DiceKriging and DiceEvaluation packages with
794 minor modifications by TLE. The code for the main analysis for sea-level change at 2100 is
795 provided.

796

797 **Data availability**

798 Simulations of the LIG and Pliocene, 1992-2017 mean and 2100 for all DP16 ensemble
799 members are provided in the Supplementary Materials. Projections at 2500 for the subset of
800 the ensemble passing their calibration are available also in the Supplementary Materials of
801 DeConto and Pollard (2016).

802

803 **Methods References**

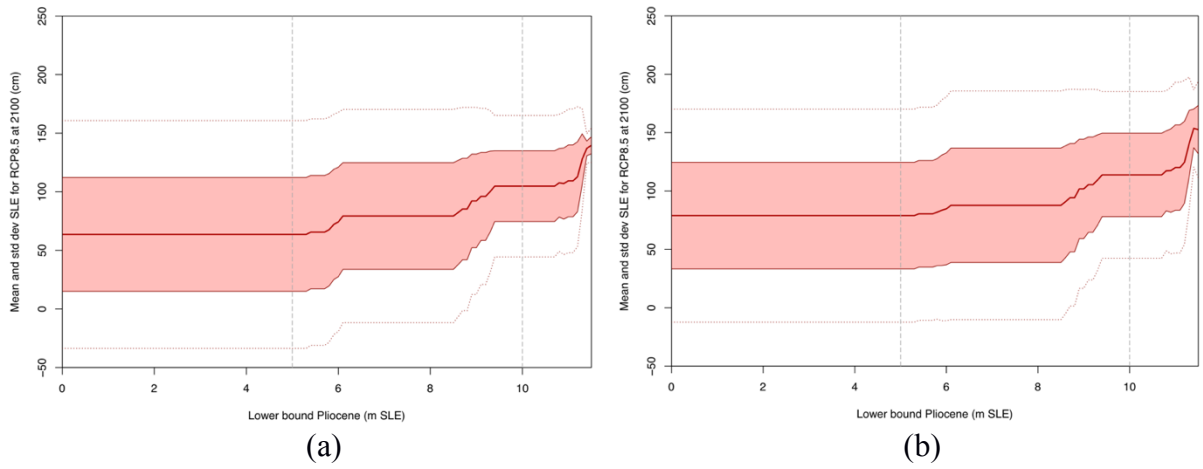
804

- 805 46. O'Hagan, A. Bayesian analysis of computer code outputs: A tutorial. *Reliability*
806 *Engineering and System Safety* 91, 1290–1300 (2006).
- 807 47. Sweet, W. V. *et al.* GLOBAL AND REGIONAL SEA-LEVEL RISE
808 SCENARIOS FOR THE UNITED STATES. 1–75 (2017).
- 809 48. Williamson, D. *et al.* History matching for exploring and reducing climate model

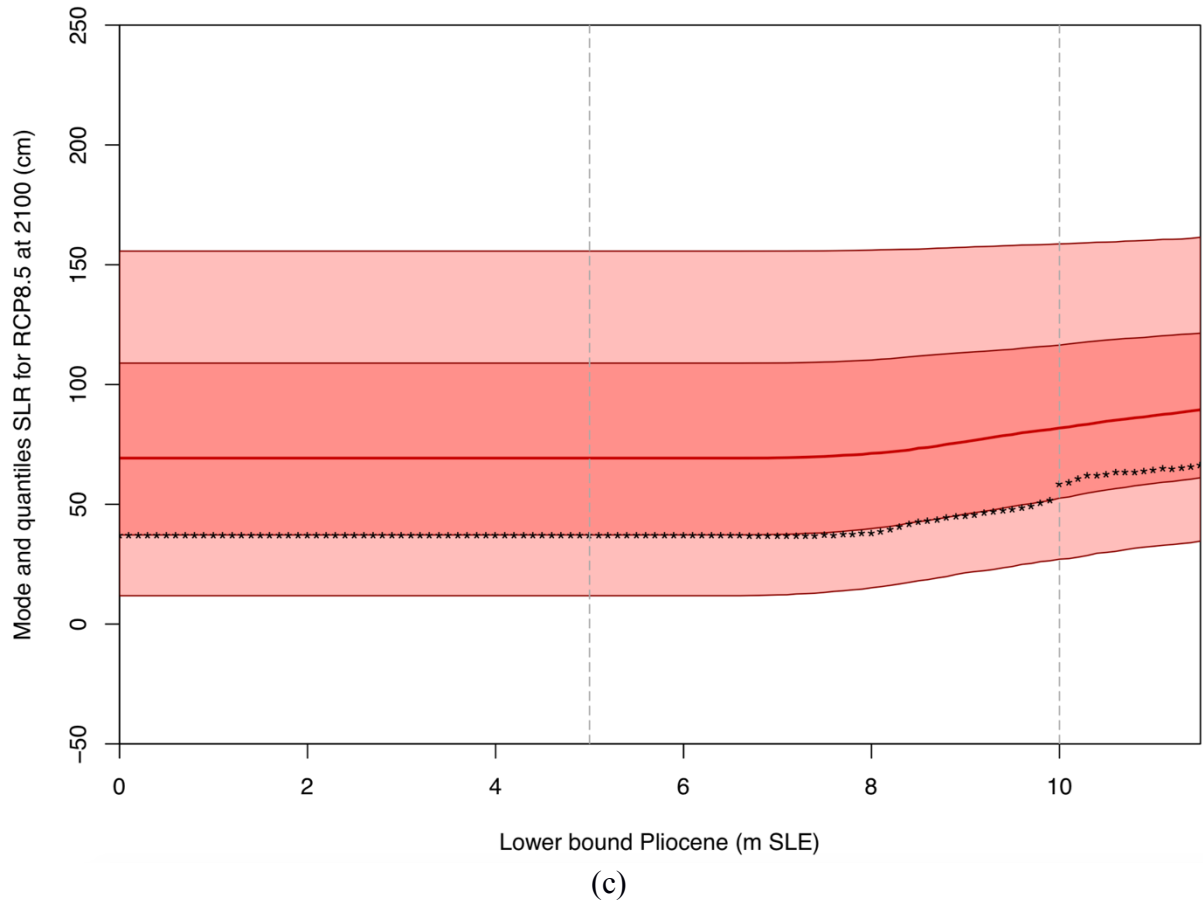
- 810 parameter space using observations and a large perturbed physics ensemble.
811 *Climate Dynamics* 41, 1703–1729 (2013).
- 812 49. Dutton, A. *et al.* Sea-level rise due to polar ice-sheet mass loss during past warm
813 periods. *Science* 349, aaa4019–aaa4019 (2015).
- 814 50. Vernon, I., Goldstein, M. & Bower, R. G. Galaxy Formation: a Bayesian
815 Uncertainty Analysis. *Bayesian Analysis* 5, 619–669 (2010).
- 816

817 **Extended Data**

818



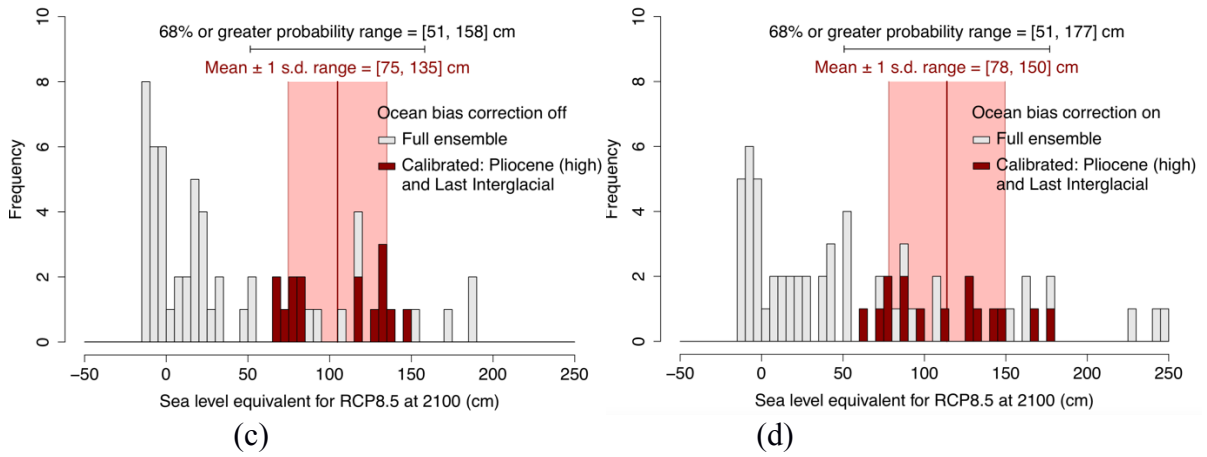
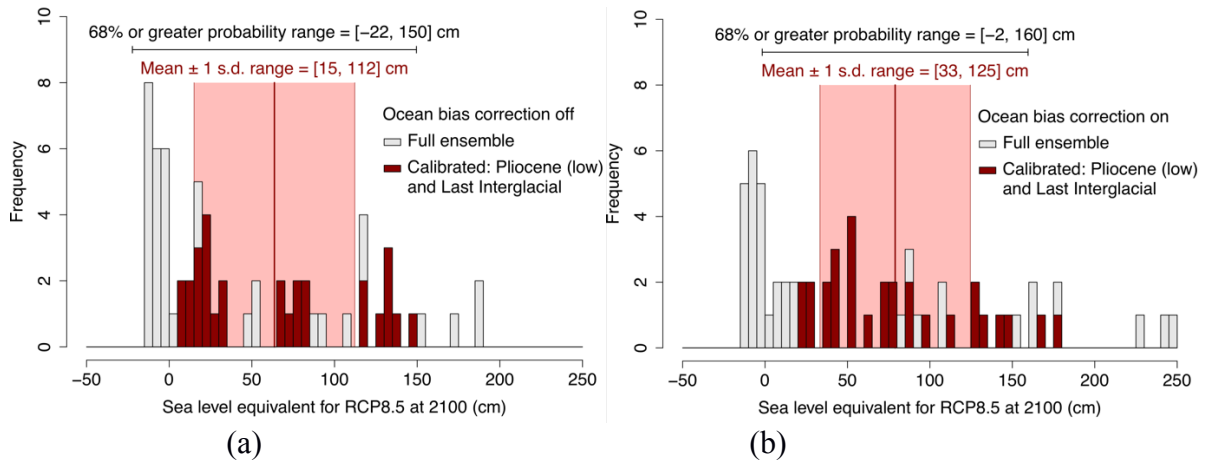
819
820
821



822
823
824
825
826
827
828
829
830

Extended Data Figure 1. Sensitivity of DeConto and Pollard RCP8.5 projections to Pliocene data lower bound. DeConto and Pollard (2016) BiasUncorrected (a) and BiasCorrected (b) projections for Antarctic sea-level contribution by 2100 under RCP8.5 as a function of the lower bound of the Pliocene data range. Mean \pm 1 s.d. range shown as central solid line with pink shading; mean \pm 2 s.d. range as dotted line. (c) Sensitivity of emulated projections for RCP8.5 at 2100 with MICI from this study: [5, 25, 50, 75, 95]th percentiles and mode (*). Data from ref. 6.

831



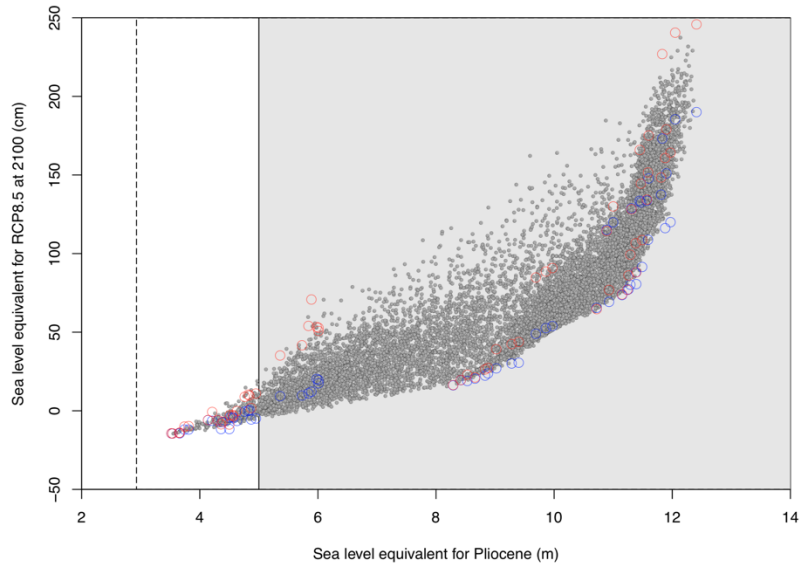
837 **Extended Data Figure 2. Shape of DeConto and Pollard RCP8.5 projection distributions.** DeConto and
838 Pollard (2016) ensemble projections for Antarctic sea-level contribution by 2100 under RCP8.5 for their four
839 variants, LowPliocene BiasUncorrected (a) and BiasCorrected (b), and High Pliocene similarly (c, d), showing
840 the full 64-member ensemble and the subset selected by calibrating with Pliocene and Last Interglacial sea-level
841 reconstructions. The mean \pm 1 s.d. range of the ensemble is shown as a solid red line with pink shading, and the
842 68% or greater probability interval is shown as a horizontal black line (see main text and Methods for more
843 details). Data from ref. 6.

844

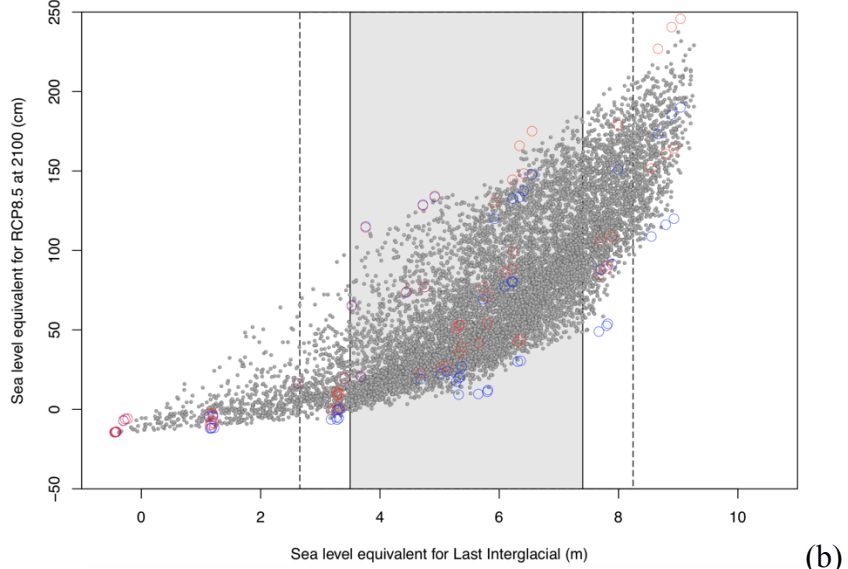
845

846

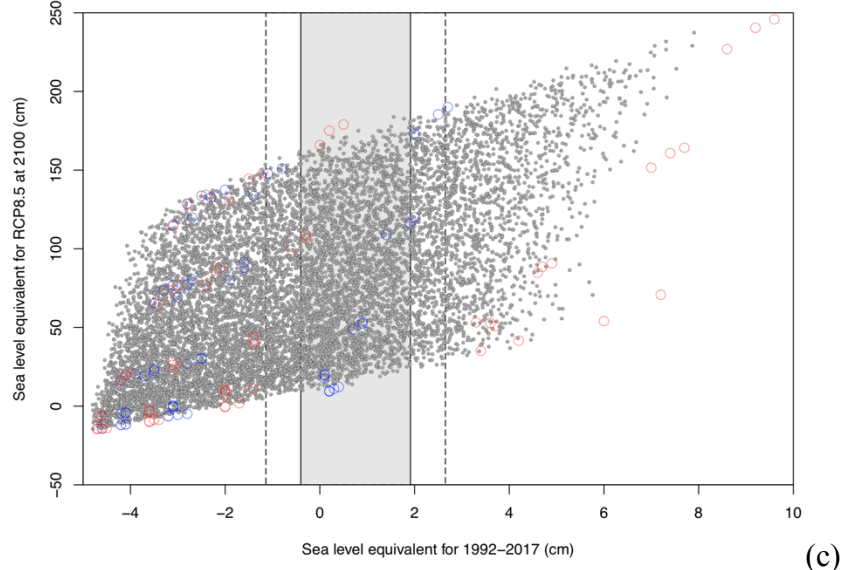
847



848



849



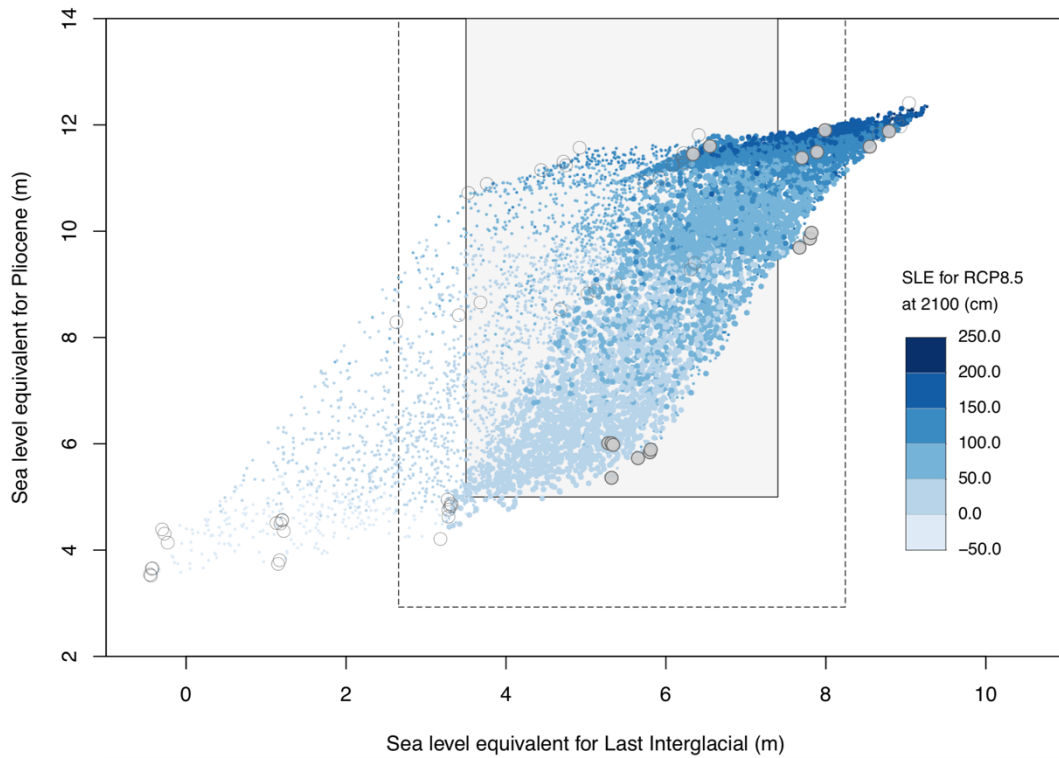
850

851

852

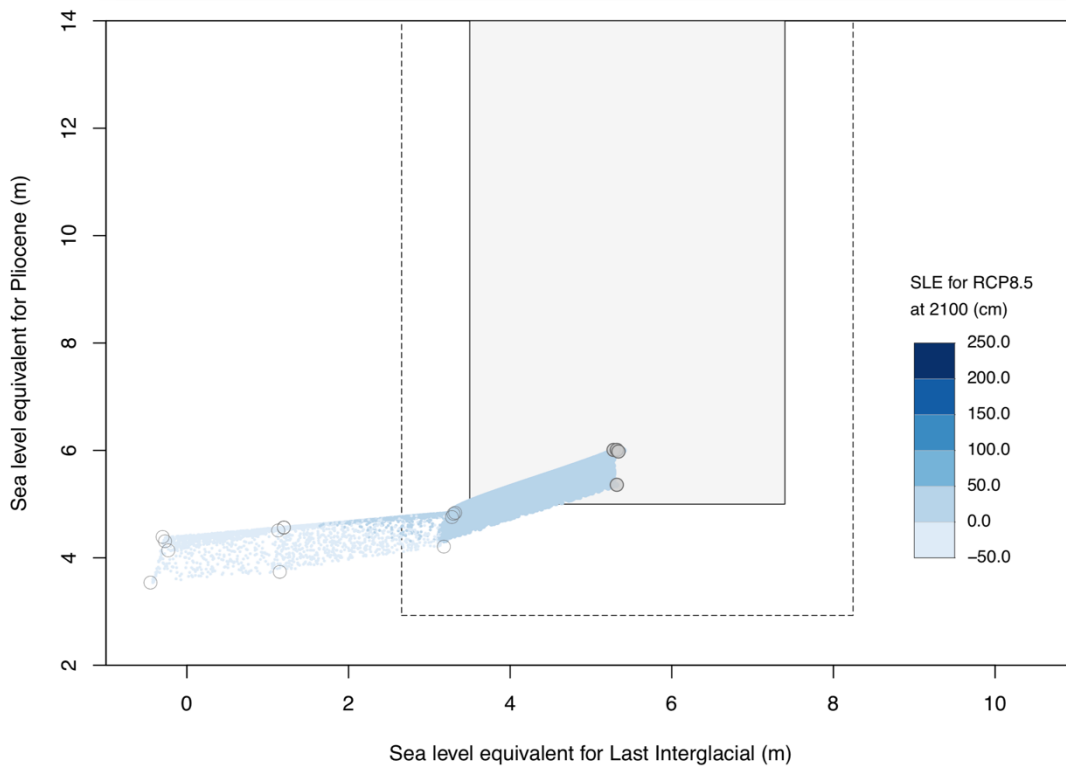
Extended Data Figure 3. Relationships between RCP8.5 projections and past sea-level changes. Sea-level contribution at 2100 under RCP8.5 versus (a) Pliocene sea-level change; (b) Last Interglacial sea-level change;

853 (c) sea-level change from 1992-2017, for the emulator (small grey dots) and DP16 simulator (large open circles)
854 with ocean bias correction off (blue) and on (red). Grey shading indicates the range of the mean plus or minus 3
855 times the observational error; the dashed line indicates 3 times the combined observational and model error.
856 Data from refs. 6 and 25 and supplementary simulations by R. DeConto (pers. comm.) (see Methods).
857
858



859

(a)



860

(b)

861 **Extended Data Figure 4. Relationship between past and future sea-level changes with and without MICI.**

862 Simulator ensemble (large grey circles), and emulated ensembles (small blue circles) with (a) cliff instability

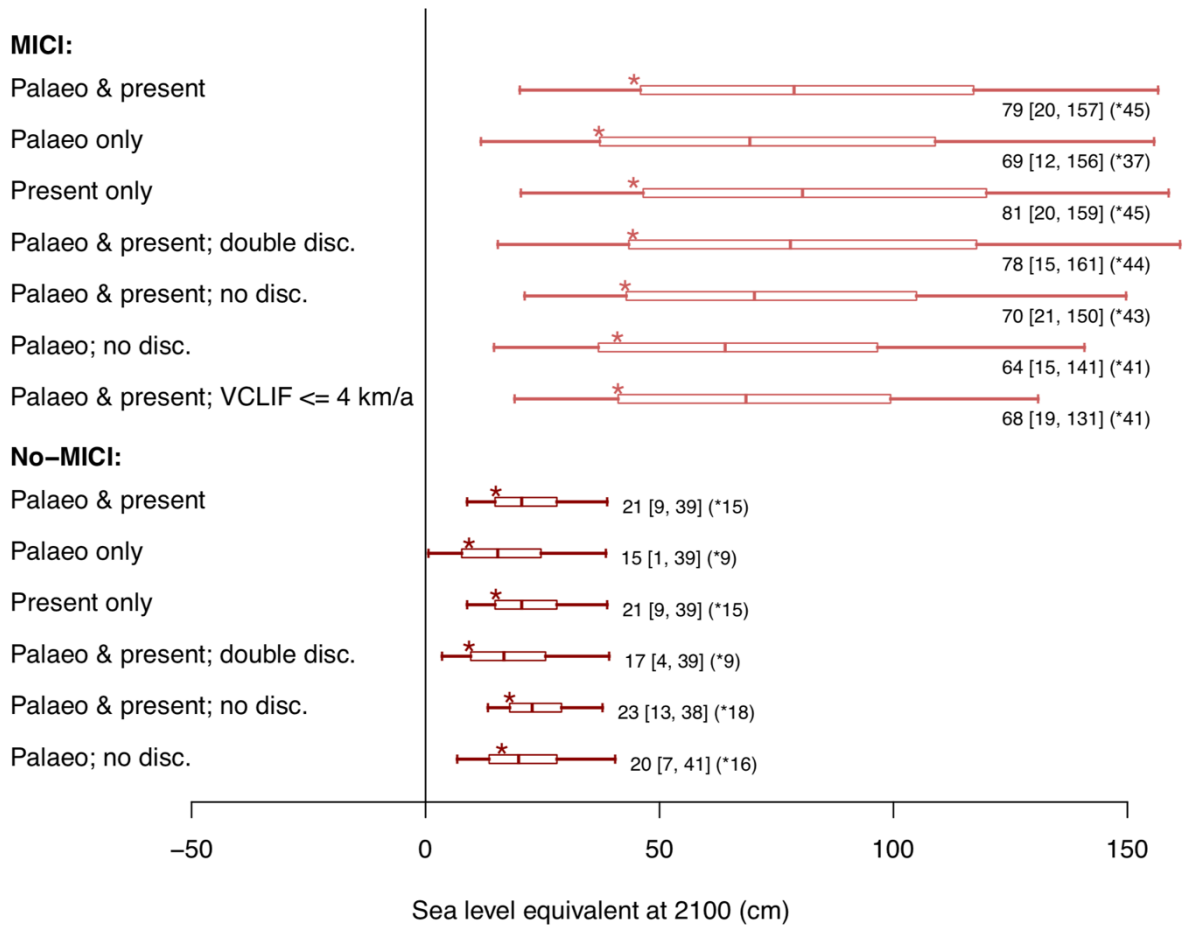
863 and (b) no cliff instability, showing Pliocene versus Last Interglacial sea-level changes. Emulator points are

864 shaded blue by sea-level contribution at 2100 under RCP8.5 (darkest is highest contribution). Large emulator

865 points and filled simulator points pass the 1992-2017 calibration. Shaded rectangle indicates bounds of DP16

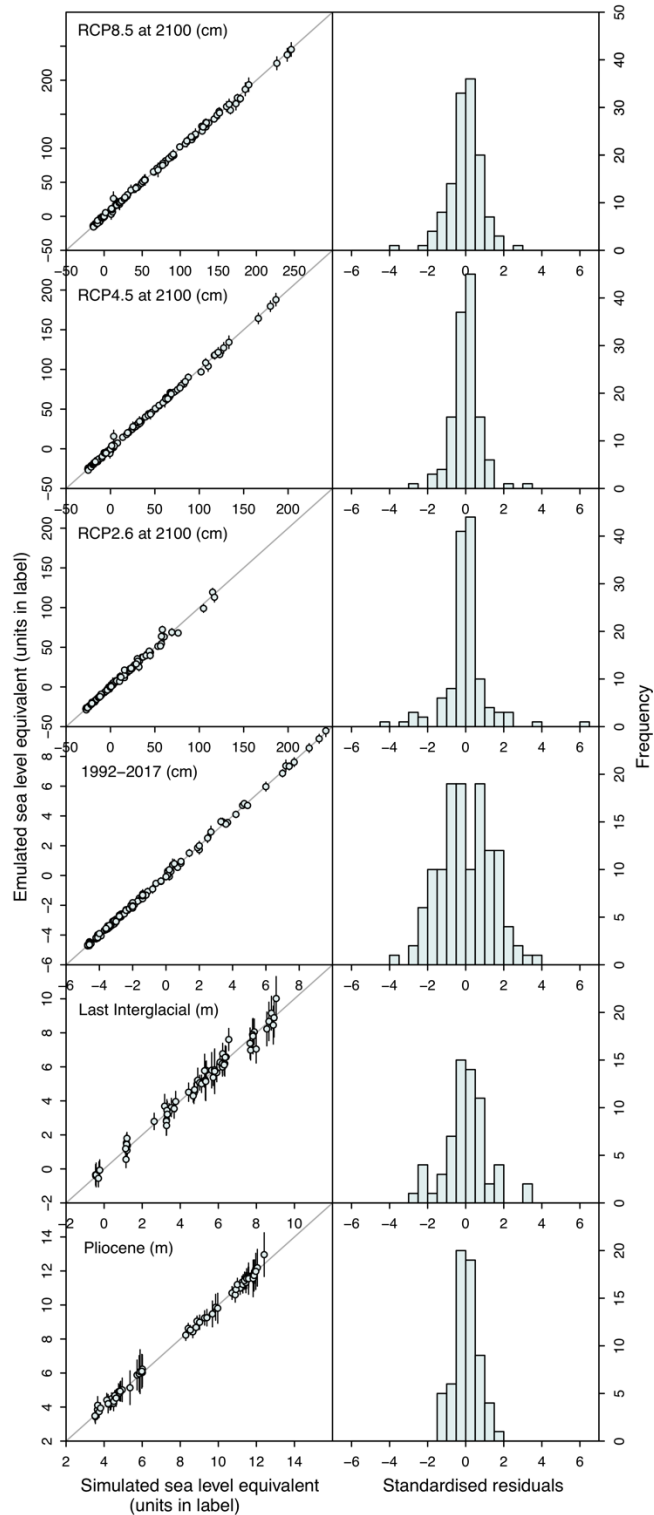
866 LowPliocene and Last Interglacial palaeodata constraints; dashed box shows bounds of palaeodata constraints in

867 this study, i.e. including model error. Data from refs. 6 and 25 and supplementary simulations by R. DeConto
868 (pers. comm.) (see Methods).
869



870

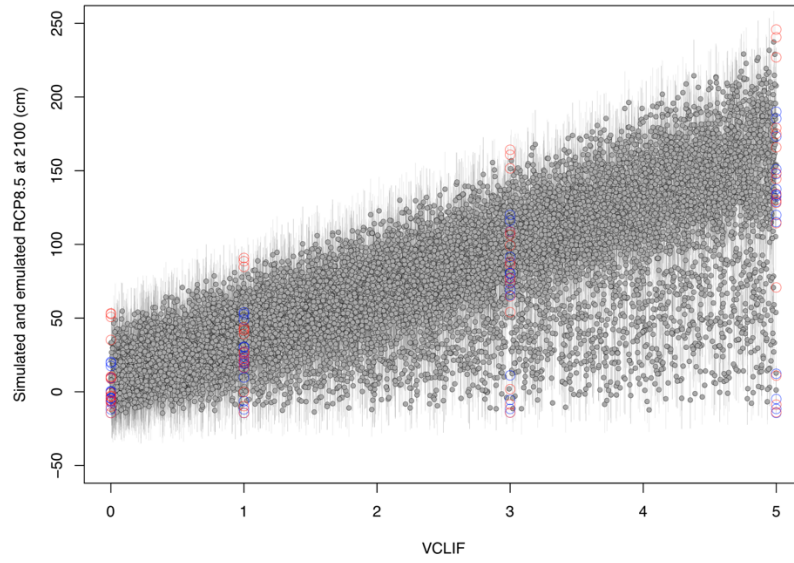
871 **Extended Data Figure 5. Sensitivity of RCP8.5 projections to MICI and calibration choices.** Projections for
 872 RCP8.5 at 2100, with and without MICI, for different combinations of calibration eras (palaeo: Pliocene and
 873 LIG; present: 1992-2017) and model discrepancy (with and without). Box and whiskers show the [5, 25, 50, 75,
 874 95]th percentiles; star shows the mode. Numbers show the median, [5th, 95th] percentiles and mode (*). Data
 875 from refs. 6 and 25 and supplementary simulations by R. DeConto (pers. comm.) (see Methods).



876

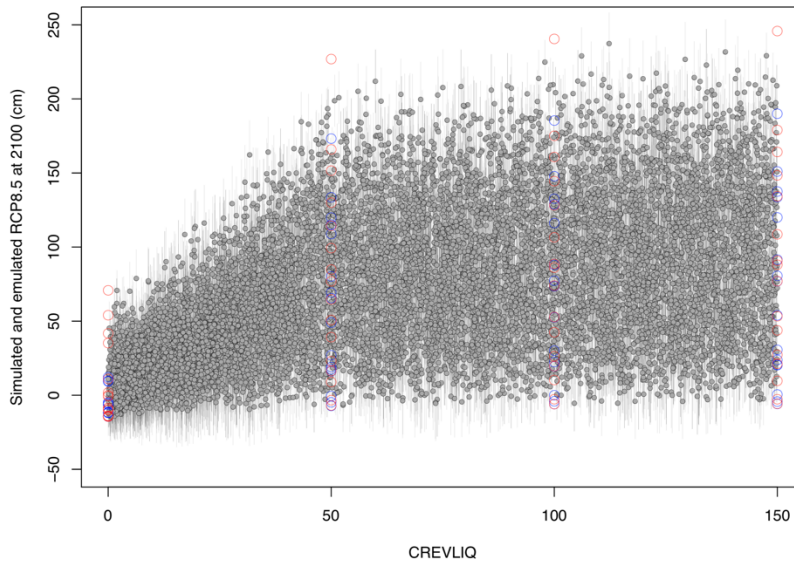
877 **Extended Data Figure 6. Emulator validation.** Left column: Emulator prediction versus simulation for each
 878 ensemble member in turn, with the emulator fitted to the other 63 ensemble members, for each of the six outputs
 879 used for building and validating emulator structure: RCP8.5, RCP4.5, and RCP2.6 sea-level contribution at
 880 2100; 1992-2017 contribution; Last Interglacial; and Pliocene. Vertical error bars show 95% credibility
 881 intervals. Right column: Difference between emulator predictions and simulations, calculated as in Extended
 882 Data Figure 7, standardised by emulator error, for the same six outputs. Values falling mostly between ± 2

883 indicate the emulator has adequate uncertainty estimates. Data from ref. 6 and supplementary simulations by R.
884 DeConto (pers. comm.) (see Methods).
885



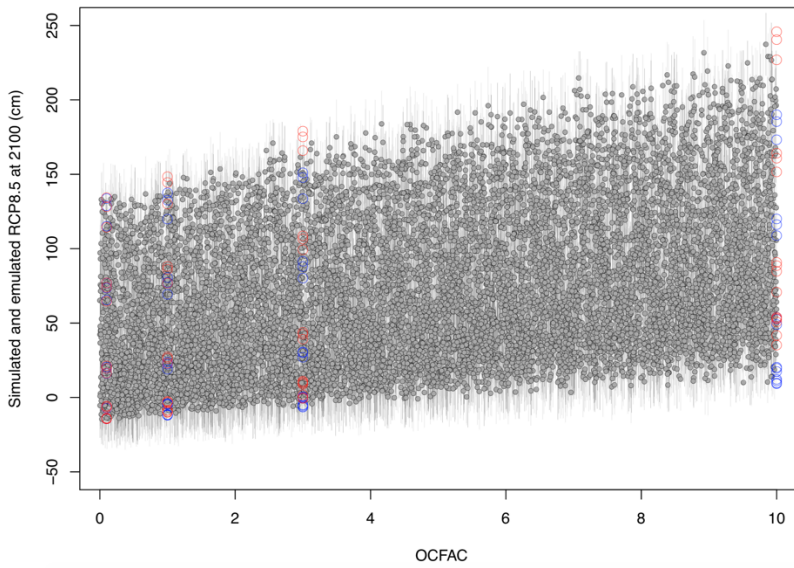
886

(a)



887

(b)



888

(c)

889

Extended Data Figure 7. Sensitivity of RCP8.5 projections to model parameters. Sea-level contribution at

890

2100 under RCP8.5 versus VCLIF (a), CREVLIQ (b) and OCFAC (c) parameters for emulator (small grey dots

891 with error bars) and simulator (large open circles: BiasUncorrected blue, BiasCorrected red). Data from ref. 6
892 and supplementary simulations by R. DeConto (pers. comm.) (see Methods).